



FACULTY OF SCIENCE AND TECHNOLOGY  
BACHELOR'S THESIS

Study programme / specialisation:  
Bachelor of Science in Petroleum  
Technology

The *spring* semester, 2023

Open

Author:

Karoline Sele

Supervisor at UiS:  
Arild Saasen

Co-supervisor:

Jorunn H. Vrålstad

External supervisor(s):

Karl Ronny Klungtvedt

Thesis title:

Lost Circulation Material Impact on Water-Based Drilling Fluids' Viscous Properties:  
Herschel-Bulkley Fluid Characterization using Dimensionless Shear Rates

Credits (ECTS): 20

Keywords: Geothermal wells; Petroleum  
Wells; Herschel-Bulkley fluids.

Pages: 40  
+ appendix: 25

Stavanger, 15.05.23

# List of Contents

Nomenclature.....	4
List of Tables.....	5
List of Figures .....	6
Abstract .....	8
<b>1 Introduction.....</b>	<b>9</b>
<b>2 Theory .....</b>	<b>14</b>
<b>2.1 Fluid Mixing .....</b>	<b>14</b>
<b>2.2 Rheology Properties .....</b>	<b>17</b>
<b>2.3 Fluid Loss.....</b>	<b>17</b>
<b>3 Experimental Work, Results and Discussion .....</b>	<b>19</b>
<b>3.1 Viscosity Parameters .....</b>	<b>19</b>
<b>3.2 Fluid Loss.....</b>	<b>25</b>
<b>3.3 Thermal and Mechanical Wear .....</b>	<b>31</b>
<b>4 Sources of Error .....</b>	<b>34</b>
<b>5 Economic Overview and Environmental Accounting .....</b>	<b>37</b>
<b>5.1 Economic Overview .....</b>	<b>37</b>
<b>5.2 Environmental Accounting .....</b>	<b>37</b>
<b>6 Conclusion .....</b>	<b>38</b>
<b>7 References .....</b>	<b>39</b>
<b>8 Appendix A .....</b>	<b>41</b>
<b>9 Appendix B .....</b>	<b>43</b>
<b>10 Appendix C .....</b>	<b>46</b>
<b>11 Appendix D .....</b>	<b>49</b>
<b>12 Appendix E.....</b>	<b>53</b>
<b>13 Appendix F .....</b>	<b>54</b>
<b>14 Appendix G:.....</b>	<b>55</b>

**15 Appendix H ..... 57**  
**16 Appendix I..... 63**

## **Nomenclature**

WBM – Water-Based Mud

OBM – Oil-Based Mud

LPLT – Low Pressure Low Temperature

HTHP – High Temperature High Pressure

PLONOR – Pose Little or No Effects to the Environment

LC – Lost Circulation

LCM – Loss Circulation Material

BHR – Before Hot Rolling

AHR – After Hot Rolling

PV – Plastic Viscosity

AV – Apparent Viscosity

EMC – European Mud Company

## List of Tables

<i>Table 3.1 Dimensionless shear rate based on Herschel-Bulkley parameters of Fluids 1-18 and Base Fluid.</i>	24
<i>Table 3.2 Filter Cakes for Base Fluid and Fluids containing different concentration of Calcium carbonate.</i>	29
<i>Table 3.3 Filter Cakes for Base Fluid and fluids containing starch.</i>	30
<i>Table 4.1 Base Fluid Before Hot Rolling (Appendix G) and its uncertainties.</i>	35
<i>Table 4.2 Base Fluid After Hot Rolling (Appendix G) and its uncertainties</i>	36
<i>Table 8.1: A-1 Name of mixtures and added different size Calcium carbonate concentration.</i>	41
<i>Table 8.2 A-2: Name of mixtures with different Calcium carbonate concentration for size &lt;math&gt; &lt; 53\mu\text{m}&lt;/math&gt;.</i>	41
<i>Table 8.3 A-3: Name of mixtures and added different starch sample 11-16.</i>	42
<i>Table 8.4 A-4: Name of mixtures and added different starch and Calcium carbonate</i>	42
<i>Table 9.1 B-1: Recipe and mixing sequence for samples 1-3 in grams unless stated otherwise.</i>	43
<i>Table 9.2 B-2: Recipe and mixing sequence for samples 11-16 in grams unless stated otherwise.</i>	44
<i>Table 9.3 B-3: Recipe and mixing sequence for samples 18-19 in grams unless stated otherwise.</i>	45
<i>Table 10.1 C-1: OFITE Calibration Fluid.</i>	46
<i>Table 10.2 C-2: Measurements of calibration fluid.</i>	48
<i>Table 14.1 G-1: Base Fluid Before Hot Rolling</i>	55
<i>Table 14.2 G-2: Base Fluid After Hot Rolling</i>	56
<i>Table 14.3 G-3: Fluid Loss Base Fluid.</i>	56

## List of Figures

Figure 2.1.1 List of Components and their functions.	14
Figure 2.1.2 Mettler Toledo PB1502-S/FACT and Hamilton Beach Mixer	16
Figure 2.1.3 Threaded steel rod used in Hot Rolling. OFITE Roller Oven 172-00-1-RC	16
Figure 2.2. 1Viscometer - OFITE 93-99 Model 800 8-Speed	17
Figure 2.3.1 LPLT test setup.	18
Figure 3.1.1 Flow curves of the fluids with different size particles of Calcium carbonate	19
Figure 3.1.2 : Flow curves of the fluids with different concentration of Calcium carbonate.	20
Figure 3.1.3 Flow Curves of the fluids with different concentrations of Calcium carbonate..	20
Figure 3.1.4 Flow Curves of the fluids with added starch.	21
Figure 3.1.5 Flow Curves of the fluids with added starch, cellulose and Calcium carbonate version 1.	22
Figure 3.1.6 Flow Curves of the fluids with added starch, cellulose and Calcium carbonate version 2.	23
Figure 3.2.1 Fluid Loss test for base fluid with three different particle sizes of Calcium carbonate and Base Fluid.	25
Figure 3.2.2 Fluid Loss test for base fluid with three different concentrations of Calcium carbonate and Base Fluid.	25
Figure 3.2.3 Fluid Loss test for base fluid with different concentrations of Calcium carbonate and Base Fluid.	26
Figure 3.2.4 Fluid Loss for Base Fluid and Fluids added Starch.	27
Figure 3.2.5 Fluid Loss for Base Fluid and fluids with added starch, cellulose and Calcium carbonate version 1.	27
Figure 3.2.6 Fluid Loss for Base Fluid and fluids with added starch, cellulose and Calcium carbonate version 1.	28
Figure 3.3.1 Flow Curves of the fluids with added N-Dril-HT BHR and AHR with and without steel rod.	31
Figure 3.3.2 Flow Curves of the fluids with added Dextrid-E BHR and AHR with and without steel rod.	31
Figure 3.3.3 Flow Curves of the fluids with added starch and Calcium carbonate BHR and AHR with and without steel rod.	32
Figure 3.3.4 Fluid Loss for Fluid 16 AHR with and without steel rod.	33
Figure 5.2.1 C-1: Measurements of calibration fluid.	48

## **Acknowledgement**

I would like to express my gratitude to several individuals who have contributed to the successful completion of this bachelor thesis. Firstly, I would like to thank my brother, Joakim Gjestland Sele, for his assistance in cutting the steel rod used in the Hot Rolling testing of fluids. Secondly, I am deeply grateful to Jorunn H. Vrålstad, the laboratory engineer, who provided me with guidance and support throughout the experimental work, including training and assistance with testing both independently and collaboratively. Thirdly, I am indebted to my supervisor from University of Stavanger, Arild Saasen, for his invaluable feedback, guidance, and support throughout the entire research process, especially during moments of confusion and uncertainty. Fourthly, I would like to extend my appreciation to Karl Ronny Klungtvedt, for his technical assistance and insightful discussions on experimental details and research articles. Additionally, I would like to acknowledge European Mud Company (ECM) for providing the various additives used in the study. Finally, I wish to express my gratitude to the Rheology Conference in Aarhus for providing me with the opportunity to present my work and for inspiring me with new ideas and approaches. Without all of their contributions, this project would not have been possible.

## Abstract

Water-based drilling fluids are commonly used in the oil and gas industry due to their favourable environmental properties and ability to effectively drill soft and unconsolidated formations. Lost circulation material (LCM) is added to prevent loss of drilling fluids into downhole formations while drilling wells. The purpose of this thesis is to investigate the effect of adding different LCMs, such as calcium carbonate and various fibres, to water-based drilling fluids. The study aims to assess the impact of fresh and worn granular and cellulose fibre-based LCMs on the viscous properties of drilling fluids. The drilling fluid's behaviour is simulated under conditions like those in the well, both at high temperatures and wear due to circulation through the nozzles. The Hot Rolling method is used to determine the drilling fluid's ability to withstand thermal wear, and a steel rod is placed in the Hot Rolling cell to simulate mechanical wear. The study also assesses the effectiveness of LCM additives in reducing lost circulation downtime and identifies the most cost-effective LCM materials for use in the North Sea. The thesis concludes with recommendations for LCM additives that provide improved drilling fluid performance and reduce downtime caused by lost circulation.

18 samples of water-based drilling fluids with added LCM were tested in this thesis. Calcium carbonate and fibres were added as LCM, both separate and combined. The Fluid Loss was measured by using API Low-Pressure Low-Temperature (LPLT) Filter Press from Appendix D and was performed on filter paper. Viscosity measurements were done on Ofite Viscometer for all samples.

The findings indicate that incorporating fibres into conventional drilling fluids that utilise  $\text{CaCO}_3$  as a Lost Circulation Material (LCM) can enhance their sealing properties and minimise formation damage, especially when effective filtration control polymers are present.



# 1 Introduction

To control the formation pressure, there must almost always be an overpressure in the well. The pressure in the well must be higher than the formation pressure. Due to this overpressure, the drilling fluid will be forced against the formation. When the formation is permeable, fluid is lost into the formation, and the solid components of the mud settle on the walls of the borehole, creating a filter cake. The filter cake can cause two problems: invasion of filtrate into the formation filter cake build-up (PET210, 2022). Filtrate can cause hole problems in shale and clay formations, such as borehole collapse and swelling of the borehole wall (PET210, 2022). The build-up of filter cake on the borehole wall will occur where there is loss of fluid to the formation. The thickness of the filter cake formed will depend on the amount of fluid lost to the formation and the amount of particles in the mud. Filter cake problems can lead to various issues, including differential sticking, increased torque, drag, lost circulation, and compromised cementing operations (PET210, 2022). The effects of the filter cake are formation protection, differential pressure control, wellbore strengthening and loss circulation control. When drilling fluid is forced against the permeable formation, some of the fluid is lost into the formation, while the solid components of the mud settle on the walls of the borehole, creating the filter cake.

Drilling fluid, also known as mud, is a fluid used in the oil and gas industry for drilling wells and has several important functions. One of its main tasks is to control pore pressure and prevent leakage, as well as to prevent formation water and gases from entering the well. To hinder loss of drilling fluids into downhole formations while drilling geothermal,  $CO_2$  injection or petroleum wells, lost circulation material (LCM) is added to the drilling fluids. The purpose of this thesis is to investigate the effect of adding different LCMs to water-based drilling fluids. Common additives such as calcium carbonate and various fibres were added to the fluid to study their impact. Alsaba et al (2014b) presented 7 different classifications for LCM based on their appearance and application: granular, flaky, fibrous, LCMs mixture, acid/water soluble, high fluid loss squeeze, swellable/hydratable combinations and nanoparticles. This thesis contains an assessment of the addition of fresh and worn granular and cellulose fibre based LCM on the viscous properties of drilling fluids. Water-based drilling fluids are widely used in the North Sea due to their favourable environmental properties and their ability to effectively drill through soft and unconsolidated formations commonly encountered in the region. Johan Sverdrup is an example of a field in the North Sea where water-based drilling fluids are utilised.

During drilling, drilling tools are subjected to high temperatures and pressures, and the drilling fluid helps cool the tools and provide necessary lubrication to prevent overheating. When the drilling fluid flows through the nozzles of the drilling machine, it is subjected to mechanical stress, high pressure, and high speeds which can cause the drilling fluid to become aerated, meaning it becomes mixed with air or gas. The temperature in the well can also have an impact on the drilling fluid due to thermal wear. Increased temperature in the formation can

cause changes in the chemical and physical composition of the drilling fluid, such as expansion and increased pressure, reduced viscosity, or the formation of foam. This will lead to increased wear on the drilling machine and nozzles. Souza et al (2022) found that temperature was the factor that most influenced the results obtained when testing granular and fibrous LCM, and higher temperatures led to lower filtrate volumes.

Therefore, it is important to test the drilling fluid under conditions similar to those in the well, both at high temperatures and wear due to circulation through the nozzles. To determine how the drilling fluid will behave, it is important to simulate the actual conditions in the relevant well to investigate how the drilling fluid will perform under these conditions. Klungtvedt and Saasen (2022a) found that to analyse the effectiveness of preventative treatment of LC, that the drilling fluid containing LCM additives must undergo relevant thermal and mechanical wear before being tested. Hot Rolling is a testing method used to determine whether the drilling fluid will experience thermal wear under high temperatures, but this method does not provide information on mechanical wear. Klungtvedt and Saasen (2022a) described a method where a steel rod is placed in the Hot Rolling cell, as shown in Figure 2.1.2, to simulate mechanical wear during circulation. Measurements were taken both with and without the steel rod, and the results showed that the mechanical wear had a strong impact on the drilling fluid's ability to seal, meaning the sealing ability was reduced. In this thesis, the same Hot Rolling method is used.

In the North Sea, loss of drilling fluid is a common problem due to the complex formations and high drilling pressures. The issue of lost circulation (LC) can be highly detrimental to the drilling process, potentially leading to reduced efficiency, heightened costs, and an increased risk of well collapse. Lowry et al (2022) found that LC had little effect on daily spending rates, however found differences in drilling cost per foot and drilling rate. The study found that the main monetary cost of LC is due to a loss of daily drilling efficiency, and that the need to reduce LC downtime rather than material costs. Grelland (2021) also found that in the North Sea only 1-2% of the cost of treating lost circulation was related to the LCM cost. Adding LCM can help reduce the downtime caused by LC by plugging the cracks and holes in the wellbore from drilling operation, thereby reducing LC downtime. Grelland (2021) also found that Calcium carbonate ( $\text{CaCO}_3$ ) and graphite are the materials mainly used as LCM in the North Sea, and alone or in combination they were insufficient as LCM. There are also advantages by using  $\text{CaCO}_3$  as LCM, it is easily available and cost-effective as it can be obtained both naturally and synthetically. This mineral is alkaline and increases the pH value when dissolved in water, which helps prevent corrosion of drilling tools and reduces the risk of formation damage.  $\text{CaCO}_3$  contributes to increasing the effective density of the drilling fluid, which helps maintain pressure in the formation and may increase oil and gas recovery. Another advantage of using calcium carbonate is improved formation water control. In low-permeability formations  $\text{CaCO}_3$  is ideal as LCM, as it can create a gel when mixed with water to effectively

seal leaks. It is most effective in water-based circulating fluids but can also be used in low-pressure formations.

Incorporating fibres into drilling fluids is beneficial in wells where the fluid properties need improvement, such as high-temperature of formation damage-prone wells, or where increased viscosity is needed to enhance carrying capacity. Bergsvik (2022) found that inclusion of fibre consistently gave lower fluid loss and fluids with a combination of  $\text{CaCO}_3$  and fibres gave a high degree of retained permeability and are interesting alternatives for non-damaging reservoir drilling fluids. Yang et al (2020) found that fibrous LCM developed the thickest filter cake and had a maximum slot-sealing pressure of approximately 500 psi, while Granular-fibre LCM had the best performance with the smoothest pressure build-up, and the maximum slot-sealing pressure could reach 2500 psi. Souza et al (2022) also found that fibrous LCM was the material with the highest filtrate volume, while blends of granular and fibrous materials presented the lowest filtrate volumes. In this thesis starch N-Dril HT, a high-temperature resistant starch, and Dextrid E, starch based viscosifier, is added to a water-based drilling fluid. The starch is added to the drilling fluid to hinder fluid loss and formation damage in the well. Alsaba et al (2014a) found that the combination of LCMs and cellulose bridging agents improved the sealing efficiency compared to LCMs without the cellulose bridging agents. They concluded that the reason was due to the fibres and cellulose bridging agents' irregularity in particle shapes and their degree of deformability, as well as their wide range of particle sizes. Klungtvedt and Saasen (2023) found that when cellulose particles were present in the filter-cake it led to reduced polymer invasion into the formation compared to when only  $\text{CaCO}_3$  was used. In this thesis  $\text{CaCO}_3$  is used at LCM both alone and in combination with fibres and cellulose bridging agent.

In this thesis, the recipe in Appendix C is used as the base for the drilling fluid, and the different additives added as shown in Table 2.1. Barite and magnesium oxide are added as weighting materials to increase the density of the drilling fluid, which is done to improve pressure control in a well and prevent blowouts. Weighting materials will also help maintain the drilling fluid's viscosity, as if the viscosity becomes too low, the drilling fluid will no longer be able to lift the cuttings. Halvorsen et al (2019) found that when barite was added to the drilling fluid sample, the shear stresses increased, this means the higher the barite content the higher shear stress. Jeennakorn et al (2019) described how drilling fluid is used to seal fractures, and how LCM particles, specifically barite, play a crucial role in this process. They found that the addition of fine particles like barite can improve force distribution and seal integrity. Potassium chloride is added as a fluid control additive to reduce the drilling fluid's tendency to filter into the formation. This is done to prevent formation damage and reduce drilling efficiency. Potassium chloride is a salt that consists of an ionic compound between positively charged potassium ions and negatively charged chloride ions. Due to this composition, the ions can affect the fluid's electrical charge by altering its electrical conductivity.

Herschel-Bulkley fluid is a type of non-Newtonian fluid, which means it does not have a constant viscosity. When viscosity is not constant, it will change with mechanical stress or deformation. This model is the most used viscosity model and combines Power-law behaviour with a yield stress. Three parameters are necessary to describe the fluid: yield stress ( $\tau_y$ ), Power-law index ( $n$ ) and consistency factor ( $k$ ) as shown in equation 1.1. The yield stress is the minimum shear stress applied to a material to create a flow. If the applied stress is less than the yield stress, the material behaves like a solid. The consistency factor ( $k$ ) is determined by the curvature exponent ( $n$ ), such that  $k = k(n)$ . However, the value of  $k$  cannot be directly measured from the fluid and must be computed through algebraic equations and is insufficient to capture all physical properties of the fluid.

$$\tau = \tau_y + k(\dot{\gamma})^n \quad (1.1)$$

Nelson and Ewoldt (2017) presented a modified Herschel-Bulkley model as shown in equation 1.2. In this equation a new parameter is introduced as  $\dot{\gamma}_c$  which represents the shear rate where the stress is equal to twice the yield stress. Saasen and Ytrehus (2020) describes problems with using this modified equation with describing drilling fluids in accordance with the API specifications. The yield stress of drilling fluids is typically very low or non-existent, making it hard or impossible to determine the shear rate at which stress is twice the yield stress. Measuring yield stress accurately in the field is challenging, and the limited number and accuracy of field viscometers make it impractical to determine this parameter.

$$\tau = \tau_y \left[ 1 + \left( \frac{\dot{\gamma}}{\dot{\gamma}_c} \right)^n \right] \quad (1.2)$$

To address the issues with equation 1.2, Saasen and Ytrehus (2020) introduced a modified version as seen in equation 1.3. They introduced two new parameters the characteristic shear rate of the flow ( $\dot{\gamma}_s$ ) and the surplus stress, ( $\tau_s$ ). The surplus stress is the additional shear stress as shown in equation 1.4. To determine the yield stress Power and Zamora (2003) introduced a method using linear regression as shown in equation 1.5. The parameter  $\theta$  is the dial reading of the measurements in accordance with API standards. The parameters are then according to the Power and Zamora method (2003):  $\tau_y$  is determined using a linear regression of the 5.11 and 10.22 1/s readings,  $\tau_s$  is determined at 102.2 1/s and  $n$  is determined at 1022 1/s. In this thesis the rheological properties of drilling fluids are described as Herschel-Bulkley fluids, with dimensionless shear rate from equations 1.3, 1.4 and 1.5. Using a dimensionless shear rate in the Herschel-Bulkley equation allows for a more accurate description of the fluid's viscosity, independent of the units used for shear rate and shear stress. The consistency index

and flow behaviour index in the Herschel-Bulkley equation are dependent on each other, but viscosity is an independent parameter that also affects the fluid's ability to resist deformation and mechanical stress. By using dimensionless shear rates, a more reliable model can be obtained to describe the fluid's rheological properties. The reliability of the model is shown by comparing the model's predicted values with experimental data. The aim of this thesis is to investigate the correlation between the theoretical model and the actual experimental data obtained from the experiments.

$$\tau = \tau_y + \tau_s \left( \frac{\dot{\gamma}}{\dot{\gamma}_s} \right)^n \quad (1.3)$$

$$\tau_s = \tau - \tau_y \quad (1.4)$$

$$\tau_y = 0.511 * \theta_0 \quad (1.5)$$

The objectives of the study were to investigate:

- The impact of fluids with varying CaCO<sub>3</sub> particle sizes as LCM on fluid loss, formation damage, and polymer concentration in the filtrate.
- Investigating the effect of using a blend of CaCO<sub>3</sub> and fibre as LCM on fluid loss, formation damage, and polymer concentration in the filtrate.
- To investigate the upper limit for the added LCM, beyond which fluid loss increases when maximum amount of LCM added is reached.
- Using a modified model of Herschel-Bulkley to describe drilling fluids.

## 2 Theory

### 2.1 Fluid Mixing

In this thesis, multiple tests were concluded on a water-based drilling fluid with different LCM added. The components used in the samples are listed in Table 2-1. During laboratory experiments involving drilling fluids, 350 mL of the fluid is used to represent one barrel (bbl) of fluid used in oil fields. This makes it practical during mixing, as 1 gram of fluid in the lab will be equivalent to 1 pound per barrel (lbs/bbl). Therefore, the sample size used for fluid mixing in the experiments is 350 mL. For simplicity, the components of the drilling fluid are reported in pounds per barrel (lbs/bbl) in the results and discussion section of this thesis. The recipes in mixing order for all drilling fluids and pills are attached in Appendix C.

Figure 2.1.1 List of Components and their functions.

Component	Description/function	Density (g/cm <sup>3</sup> )
Hydrogen oxide, H <sub>2</sub> O, water	Solvent and a carrier for other components in the fluid.	1
Sodium carbonate, Na <sub>2</sub> CO <sub>3</sub> , soda ash	Controlling alkalinity in fluid.	1
Sodium hydroxide, NaOH, caustic soda	Controlling alkalinity in fluid.	1
Xanthan gum, XC	Viscosity regulator in fluid.	0,95
Magnesium oxide, MgO	Controlling alkalinity in fluid.	3,58
Sodium chloride, NaCl, salt	Controlling alkalinity in fluid.	2,71
Barite, BaSO <sub>4</sub>	Weighting agent: controlling the weight. viscosity and increase the density of the fluid.	4,5
Calcium carbonate, CaCO <sub>3</sub> , <23μm	Bridging agents, preventing fluid invasion and weighting materials in the fluid. The smaller particle sizes are used to improve fluid density.	2,7
Calcium carbonate, CaCO <sub>3</sub> , D50=50μm	Bridging agents, preventing fluid invasion and weighting materials in the fluid. The smaller particle	2,7

	sizes are used to improve fluid density.	
Calcium carbonate, $\text{CaCO}_3$ , $<53\mu\text{m}$	Bridging agents, preventing fluid invasion and weighting materials in the fluid. Control rheological properties of the fluid such as yield point and gel strength.	2,7
Starch N - Dril HT	Starch-based polymer that increases the viscosity of the fluid.	0,95
Starch Dextrid - E	Starch-based polymer that increases the viscosity of the fluid.	0,95
Auraoat UF	A cellulose-based bridging agent made from fibres.	1

All the components were weighed on a Mettler Toledo weight following the recipes in appendix A. Throughout the experimental process, all tests were conducted in duplicate. Initially, parallel 1 and parallel 2 were mixed separately in Hamilton mixers for 5 minutes at high speed. Then they both were mixed together in a large breaker to make one fluid, then separated again into two separate containers, representing parallel 1 and parallel 2. This method was employed to reduce uncertainty associated with mixing and blending of the drilling fluid. Following the mixing process, parallel 1 and parallel 2 are separately placed in a viscometer, where the fluids are measured at various speeds following the API procedure from Appendix B. After these measurements, parallel 1 and parallel 2 were each placed into separate cells to undergo Hot Rolling at 90 °C for 16 hours, this is done to simulate the actual field conditions in a reservoir. The cells are hot-rolled at 90 °C in this study, although the common practice is to hot-roll at 112-120 °C, because starch degrades at temperatures above 110 °C and this would impact the test results on the drilling fluid with added starch.

All tests in this study were conducted at room temperature to maintain consistency in the temperature-dependent viscosity measurements. After Hot Rolling, the cells were allowed to stand in a fume hood for 3 hours to cool down to room temperature. To perform viscosity measurements, the fluids in the cells were mixed for 10 minutes using a Hamilton Beach mixer before repeating the viscometer measurements. This process was repeated for all tests in the study. The equipment used are shown in Figure 2.1.1.



*Figure 2.1.2 Mettler Toledo PB1502-S/FACT and Hamilton Beach Mixer*

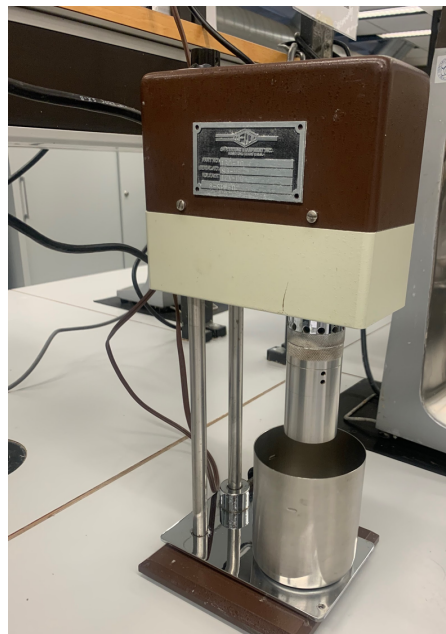


*Figure 2.1.3 Threaded steel rod used in Hot Rolling. OFITE Roller Oven 172-00-1-RC*



## 2.2 Rheology Properties

The drilling fluid is placed in the annular space between two concentric cylinders. The outer cylinder is called the rotor sleeve and it is driven at a constant rotational velocity. This rotation generates torque on the inner cylinder, called the bob, as it interacts with the drilling fluid (API from Appendix B). To limit the movement of the bob, a torsion spring is used, and a dial attached to the bob displays its displacement. By gauging the displacement of the bob, the viscometer can determine the viscosity of the drilling fluid. The two parallels were subsequently measured separately in a viscometer, following the API Procedure from Appendix B, at speeds of 600, 300, 200, 100, 60, 30, 6, and 3 rpm, with measurements being conducted from highest to lowest speed.



*Figure 2.2. Viscometer - OFITE 93-99 Model 800 8-Speed*

## 2.3 Fluid Loss

To measure the fluid loss in the two parallels a LPLT was used following the API procedure from appendix C. The LPLT test is based on surface condition and will not simulate the downhole conditions. However, the LPLT test can still provide valuable information about fluid loss and is a simpler and less expensive test to perform than the HPHT. It is important to address that wellbore temperature and pressure can dramatically change the properties of a drilling fluid, and therefore the results of the LPLT test cannot replicate downhole conditions. The aim of the test is to measure the filtration of mud with ambient temperature and 100 psi differential pressure. The test was conducted with readings recorded at 5 minutes intervals for

30 minutes. To ensure accurate measurement of fluid loss, a filter paper with a pore size of 2.2  $\mu\text{m}$  is used in the fluid loss test conducted on drilling fluids containing fibres of various sizes. This was done for drilling fluids containing fibres of varying sizes. This pore size was deemed optimal efficient capture of drilling fluid particles and fibres, while allowing for unimpeded fluid flow to ensure precision in measurement. Utilisation of a filter paper with a larger pore size could result in blockages and hence, inaccurate measurements of fluid loss.



*Figure 2.3.1 LPLT test setup.*

### 3 Experimental Work, Results and Discussion

This section of the thesis comprises three parts: Viscosity parameters, Fluid Loss, and Mechanical and Thermal Wear. The first part presents experimental data for a base fluid supplemented with various LCMs (see Appendix A) modelled as Herschel Bulkley fluids using Equation 1.3. The second part consists of fluid loss tests conducted on the fluids containing different LCMs. The third part encompasses both viscosity measurements and fluid loss tests conducted with and without mechanical wear. This section investigates the impact of thermal and mechanical wear on the fluids. All data in the graphs were plotted using Python code in Appendix I.

#### 3.1 Viscosity Parameters

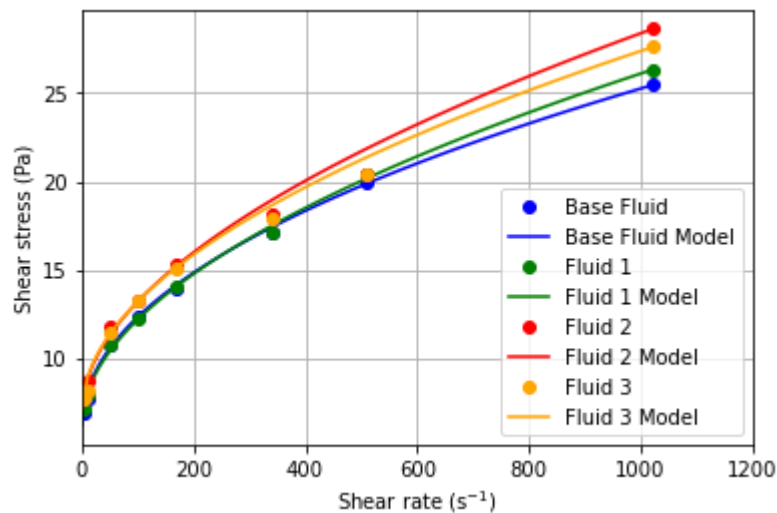


Figure 3.1.1 Flow curves of the fluids with different size particles of Calcium carbonate

With the exception of carbonate particle size, fluids 1-3 and base fluid were constructed equally. The yield stress, surplus stress, and n-value were calculated using Eq. 1.3 from the data shown in appendix B. There is little difference between the fluids, but it can be observed that Fluid 2 and 3, which contain larger particle sizes ( $<53\mu m$  and  $D50=50\mu m$ ), exhibit slightly higher values for yield stress and surplus stress as shown in Table 3. An increase in both surplus stress and yield stress for larger particle sizes of  $CaCO_3$  can be attributed to increased particle interactions. When the particles are larger in size, they have larger surface areas that can bind together more effectively. The expected result is that the larger particle sizes of  $CaCO_3$  would yield higher values, however Bergsvik (2022) found that Hot Rolling with a threaded steel rod resulted in almost total degradation of  $CaCO_3$  particles larger than  $53\mu m$  and that impacted the results in this thesis.

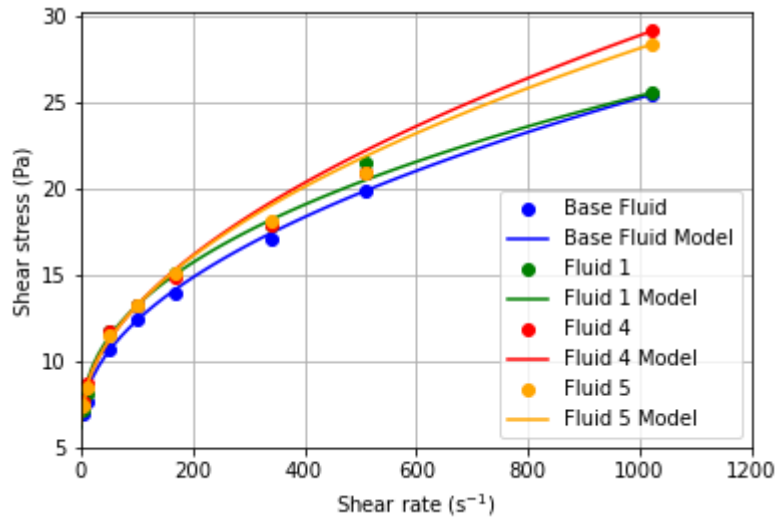


Figure 3.1.2 : Flow curves of the fluids with different concentration of Calcium carbonate.

Fig. 3-1-2 shows the plot of the viscosity measurement data for samples 1, 4, and 5. With the exception of carbonate content, these fluids were constructed equally. Fluids 1, 4 and 5 had 20, 40 and 60 g calcium carbonate per 350 mL respectively. From the data shown in Fig. 3-1-2, it seems that addition of the two larger concentrations of calcium carbonate only added to the viscosity of the fluid at higher shear rates. It is seen that the shear thinning index,  $n$ , became a bit larger for Fluids 4 and 5. This is expected as the amount of solid particles became higher for these fluids giving a higher shear rate viscosity.

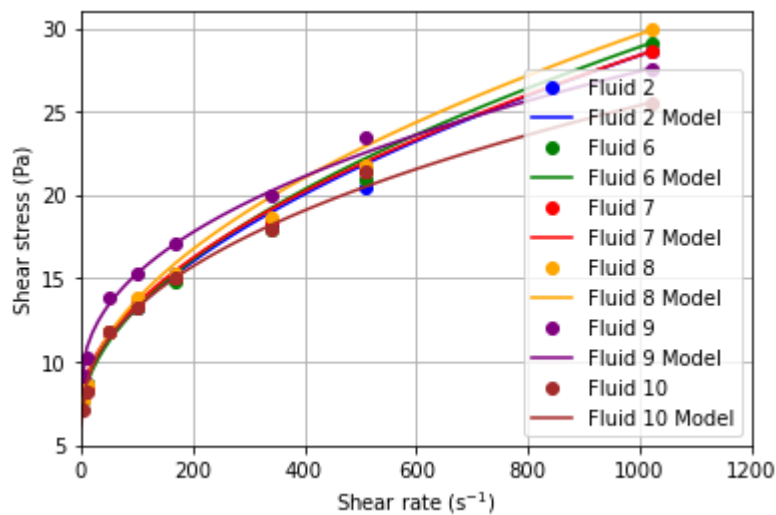


Figure 3.1.3 Flow Curves of the fluids with different concentrations of Calcium carbonate..

With the exception of carbonate concentration fluids 2, 6, 7, 8, 9 and 10 were constructed equally, and their viscosities exhibit minimal variation. Fluids 2, 6, 7, 8, 9 and 10 had 20, 40, 45, 50, 55 and 60 g calcium carbonate per 350 mL respectively. Fluid 10 containing 60 g of CaCO<sub>3</sub> had a lower viscosity than the rest of the samples. Indicating that there is a critical concentration, where the viscosity decreases instead of increasing with the increase of concentration of CaCO<sub>3</sub>.

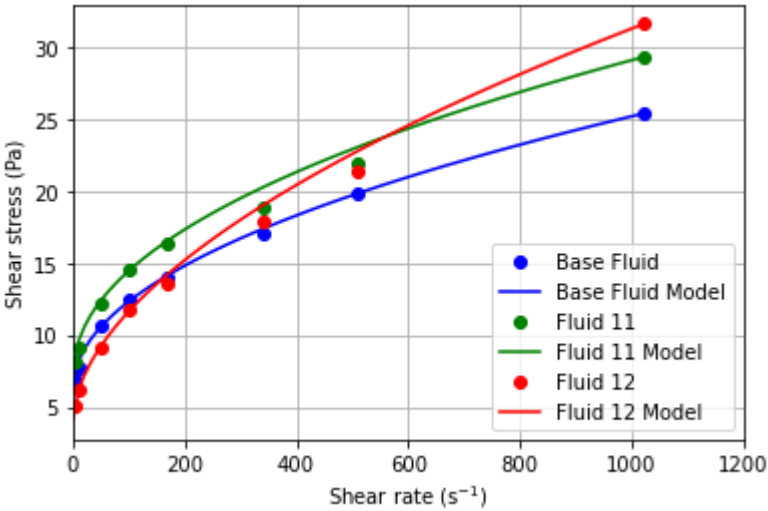


Figure 3.1.4 Flow Curves of the fluids with added starch.

Fig. 3-1-4 shows drilling fluids sample 11 and 12 with added starch and the base fluid without added LCM. Sample 11 contains 2g N-Dril HT and sample 12 contains 5g Dextrid-E, the results show a reduction in low shear viscosity and an increase in high-shear viscosity. It is seen that the shear thinning index, *n*, became a bit larger for Fluid 12. This is expected as the amount of solid particles became higher for fluid 12 (5g) giving a higher shear rate viscosity.

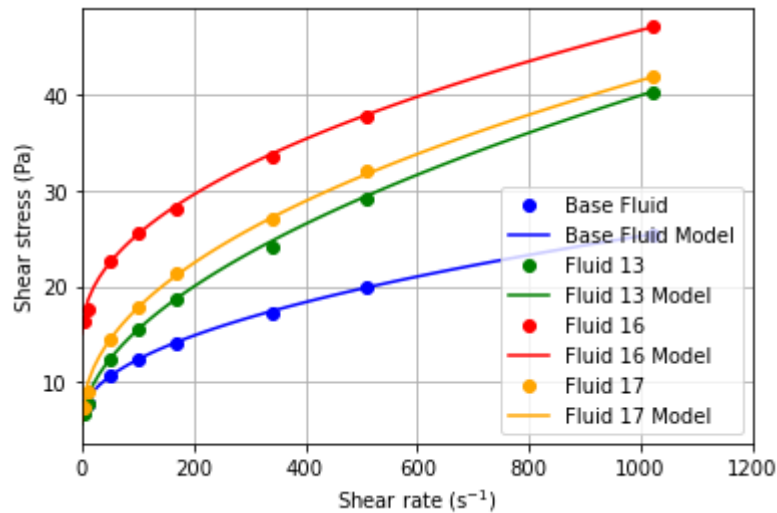
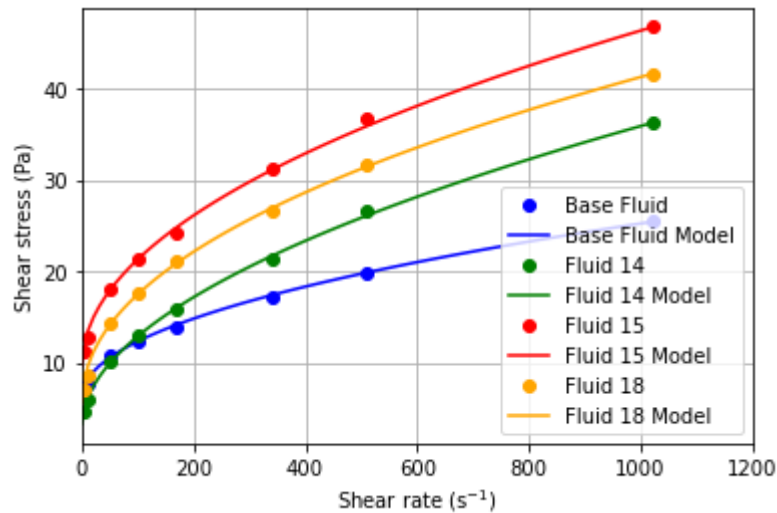


Figure 3.1.5 Flow Curves of the fluids with added starch, cellulose and Calcium carbonate version 1.

Fig 3-1-4 contains the fluids 13, 16, 17 and base fluid. Fluid 13 contains 2g N-Dril HT and 5g Dextrid-E, and the same as in Fig 3-1-3 the results show a reduction in low shear viscosity and an increase in high-shear viscosity. Fluid 16 is constructed equally as Fluid 13, with exception of 5g Auracoat UF. Auracoat UF is a cellulosic fibre mixture, and this has an impact on the viscous properties of the fluid. The yield stress and surplus stress values are higher when adding the cellulose bridging agent, it enhances the bridging capability of the fluid. This enhanced bridging action can result in increased particle interactions and stronger structural networks, leading to higher surplus stress and yield stress values. The combined presence of N-Dril HT, Dextrid-E, and Auracoat UF can create a more cohesive and robust fluid structure, leading to higher surplus stress and yield stress values compared to using only N-Dril HT and Dextrid-E as in Fluid 13. Fluid 17 is constructed equally as Fluid 16, but with addition of 40g CaCO<sub>3</sub>. When adding CaCO<sub>3</sub> to the drilling fluid combined with the starch, resulted in a decrease in viscosity. When adding more particles the expected value would be an increase in viscosity, but Klungtvedt and Saasen (2023) found that Hot Rolling caused degradation of CaCO<sub>3</sub> particles, but cellulose-based LCM showed low levels of particle size degradation. Because of the degrading of CaCO<sub>3</sub> the smaller particle sizes may result in reduced particle-particle interactions, leading to lower viscosity. While only using cellulose-based LCM as in Fluid 16 the viscosity is higher, because of low levels of particle size degradation.



*Figure 3.1.6 Flow Curves of the fluids with added starch, cellulose and Calcium carbonate version 2.*

Fig 3-1-5 contains the fluids 14, 15, 18 and base fluid and it has similar trends and resembles Fig 3-1-2. Fluid 14 and Fluid 13, Fluid 15 and Fluid 16, Fluid 18 and Fluid 17, from Fig 3-1-5 and 3-1-4 are constructed equally with the exception of starch concentration. Fluid 14 contains 3,5g N-Dril HT and 3,5g Dextrid-E, and the same as in Fig 3-4 the results show a reduction in low shear viscosity and an increase in high-shear viscosity. Fluid 15 is constructed equally as Fluid 14, with exception of 5g Auracoat UF. The yield stress and surplus stress was higher for Fluid 15 than Fluid 14, as also seen in Fig. 3-1-4.

*Table 3.1 Dimensionless shear rate based on Herschel-Bulkley parameters of Fluids 1-18 and Base Fluid.*

	<b>Yield Stress</b>	<b>Surplus Stress</b>	<b><i>n</i></b>
<b>Base Fluid</b>	6,234	6,183	0,492
<b>Fluid 1</b>	6,387	5,876	0,530
<b>Fluid 2</b>	7,154	6,132	0,544
<b>Fluid 3</b>	7,154	6,132	0,523
<b>Fluid 4</b>	6,643	6,643	0,530
<b>Fluid 5</b>	6,388	6,899	0,503
<b>Fluid 6</b>	6,643	6,643	0,530
<b>Fluid 7</b>	7,410	6,132	0,540
<b>Fluid 8</b>	6,643	7,154	0,512
<b>Fluid 9</b>	8,176	7,154	0,433
<b>Fluid 10</b>	6,132	7,154	0,434
<b>Fluid 11</b>	7,154	7,410	0,477
<b>Fluid 12</b>	4,088	7,665	0,556
<b>Fluid 13</b>	5,621	9,964	0,542
<b>Fluid 14</b>	3,322	9,709	0,530
<b>Fluid 15</b>	9,710	11,753	0,499
<b>Fluid 16</b>	15,074	10,475	0,485
<b>Fluid 17</b>	5,876	12,008	0,477
<b>Fluid 18</b>	5,621	12,009	0,477



### 3.2 Fluid Loss

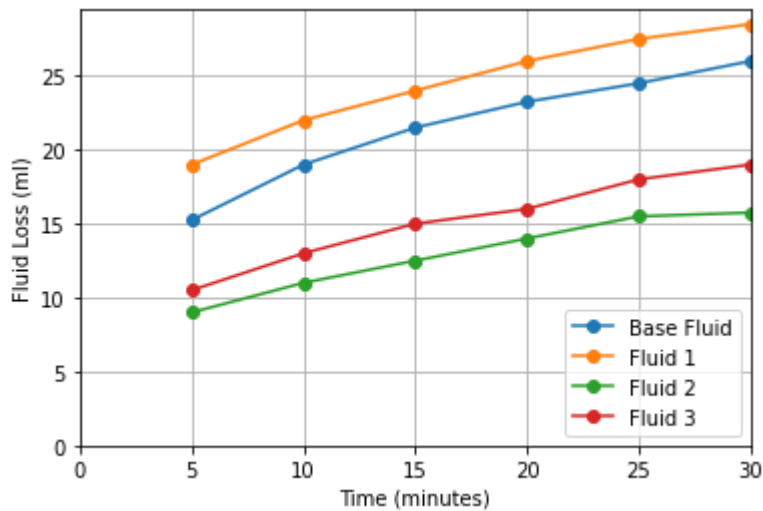


Figure 3.2.1 Fluid Loss test for base fluid with three different particle sizes of Calcium carbonate and Base Fluid.

From Figure 3-2-1, it is evident that Fluid 1, which contains the smallest particle sizes of  $\text{CaCO}_3$ , exhibits higher fluid loss compared to the Base Fluid without added LCM. One possible reason for this is that the smaller particle size leads to decreased particle-particle interactions. With fewer particle-particle interactions, the particles are unable to form an effective seal, resulting in increased fluid loss. There is minimal difference between Fluid 2 and Fluid 3, and one reason for this is that after Hot Rolling with mechanical and thermal wear, particle sizes larger than  $53\mu\text{m}$  of  $\text{CaCO}_3$  were completely degraded (Bergsvik 2022). Therefore, it is likely that the particle sizes after Hot Rolling are quite similar for Fluid 2 and Fluid 3, and they will form an equally strong seal.

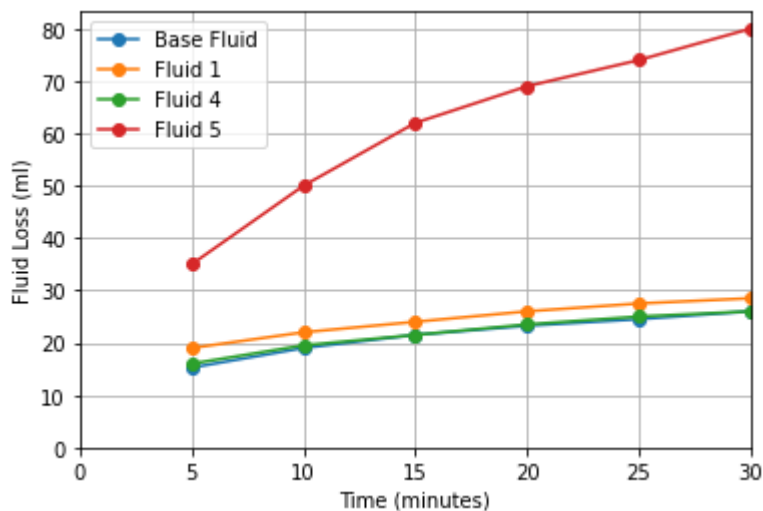


Figure 3.2.2 Fluid Loss test for base fluid with three different concentrations of Calcium carbonate and Base Fluid.

As seen in Figure 3-1-6 the plot indicates that there is a critical concentration of  $\text{CaCO}_3$  and Figure 3-2-2 shows that critical concentration even more clearly. Fluid 5 containing 60g of  $\text{CaCO}_3$  has larger volumes of Fluid Loss compared to Fluid 1 and 4 containing 20g and 40g of  $\text{CaCO}_3$ . However when the  $\text{CaCO}_3$  concentration is increased from 20g to 40g in Fluid 1 and Fluid 4, the Fluid Loss decreases. Alsaba et al (2014a) found that higher LCM concentrations generally yielded better results, but there was a critical maximum concentration beyond which no tight seal could be formed. From Figure 3-2-1 the critical maximum concentration is 60g for this drilling fluid.

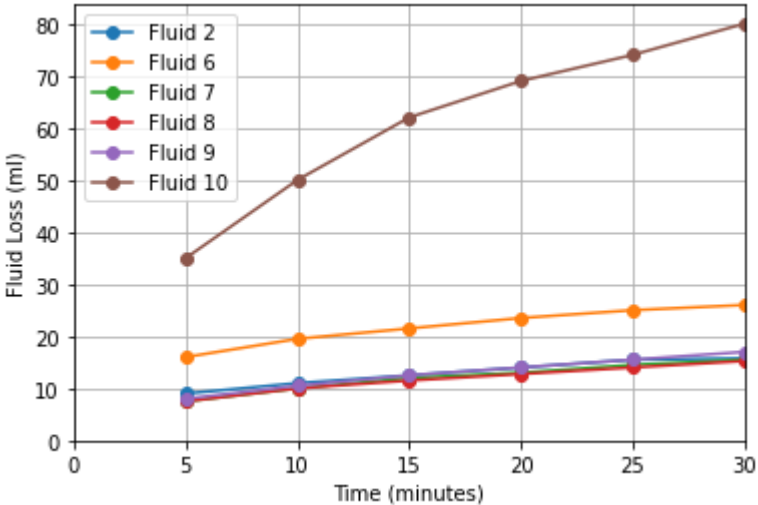


Figure 3.2.3 Fluid Loss test for base fluid with different concentrations of Calcium carbonate and Base Fluid.

Fluids 2-10 are constructed equally with exception of  $\text{CaCO}_3$  concentrations, they contain only particle size  $53\mu\text{m}$   $\text{CaCO}_3$ . The  $\text{CaCO}_3$  concentrations are 20g, 40g, 45g, 50g, 55g and 60 for Fluids 2, 6, 7, 8, 9 and 10 per 350 mL. Fluid 6 containing the smallest concentration of 20g  $\text{CaCO}_3$  has a higher Fluid Loss volume than Fluids 7-9, this is expected that higher concentrations of LCM generally yield better results. However, for Fluid 10 that contains 60g the Fluid Loss is severe, this can also be observed in Figure 3-2-2. Fritoli et al (2021) found that high concentrations of  $\text{CaCO}_3$  resulted in increased cake mass and thickness but not lower volume of filtrate, suggesting the existence of a critical concentration value above which the influence on lost circulation is minimal. The increased cake mass and thickness can be seen in Figure 3-2-6 and Fluid 10 stands out with its thick filter cake.

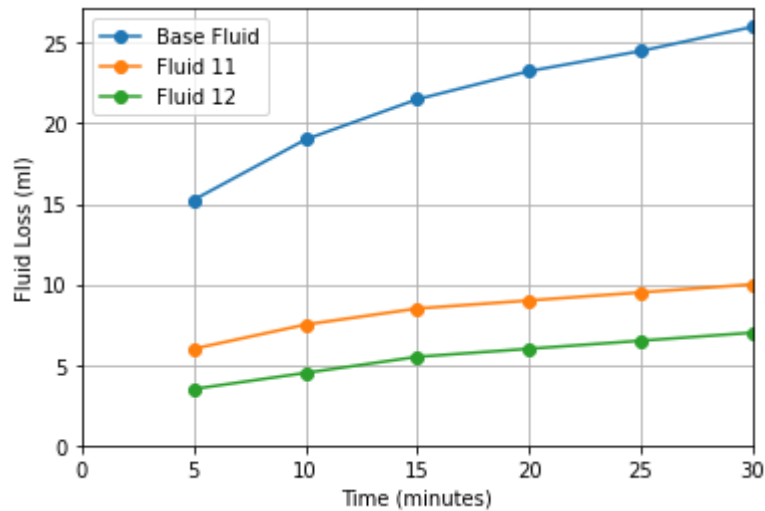


Figure 3.2.4 Fluid Loss for Base Fluid and Fluids added Starch.

Figure 3-2-5 shows the Fluid Loss for Fluids 11, 12 and Base Fluid without added LCM. All Fluids were constructed equally with the exception of the addition of various fibres in Fluid 11 and 12. Fluid 11 contains 2g N-Dril HT and Fluid 12 5g Dextrid-E. N-Dril HT is a high-temperature resistant starch while Dextrid E is another starch based viscosifier. The Fluid Loss volume significantly decreases when starch is added to the drilling fluid, as can be seen from Figure 3-2-5. Fluid 11 only contains 2g of starch, while Fluid 12 contains 5g. So, it is expected that Fluid 12 has lower filtrate volume that Fluid 11.

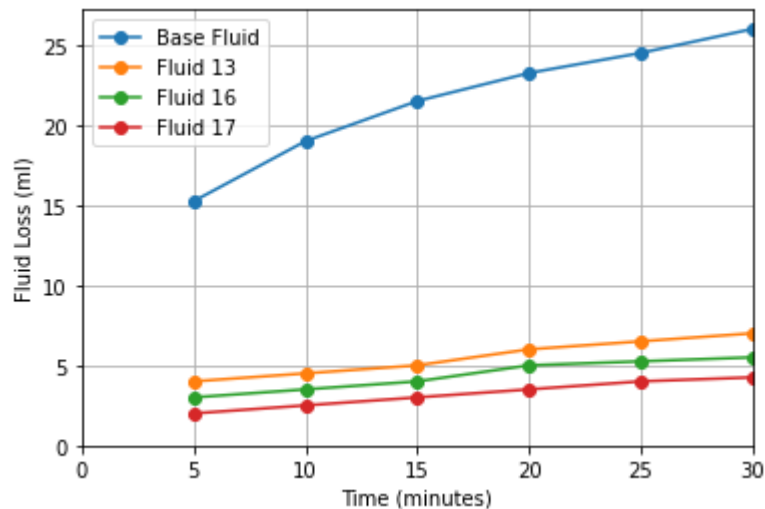


Figure 3.2.5 Fluid Loss for Base Fluid and fluids with added starch, cellulose and Calcium carbonate version 1.

Figure 3-2-5 contains a Base Fluid without added LCM and three Fluids containing fibres, cellulose and CaCO<sub>3</sub>. All fluids were constructed with the same Base-Fluid, however Fluids 13, 14 and 16 have different additives. Fluid 13 contains 2g N-Dril HT and 5g Dextrid-E, both are starch based viscosifiers. Fluid 16 is constructed the same as Fluid 13 but with the

addition of 5g Auracoat UF, a patented mixture of cellulose fibre used to hinder fluid loss and formation damage. Fluid 17 is constructed the same as Fluid 16 but with addition of 40g CaCO<sub>3</sub>, 20g CaCO<sub>3</sub> (<53µm) and 20g CaCO<sub>3</sub> (D50=50µm). The Fluid Loss for the Base Fluid is much higher than for the drilling fluids with added starch. Klungtvedt and Saasen (2022a) found that the cohesive strength of the filter cake was found to be higher with increased concentration of polymers and cellulose-based fibres. The inclusion of cellulose fibres in drilling fluids enhances the binding of polymers to the filter cake, resulting in a reduced release of polymers into the formation. This can be attributed to the polar properties of both cellulose particles and polymers, which potentially increase inter-particle adhesive and frictional forces. Figure 3-2-8 shows compact filter cakes for the samples with added starch and cellulose compared to the filter cakes in Figure 3-2-7 only containing CaCO<sub>3</sub>. Fluid 16 and 17 contains Auracoat and the results are not as significant as expected. There is a small decrease in filtrate volume, but based on studies the expected results would be a larger difference in filtrate volumes for fluids with and without cellulose as a bridging agent. While the fluid loss tests in this study were conducted at 100 psi, Klungtvedt and Saasen (2023) discovered that the most significant variations in Fluid Loss, attributed to the use of N-Dril-HT cross linked starch and Dextrid E modified starch in conjunction with Auracoat UF, which is a cellulosic fibre mixture, were observed at pressure ranges of 500-1000 psi. The Fluid Loss test performed in this thesis is at 100 psi differential pressure.

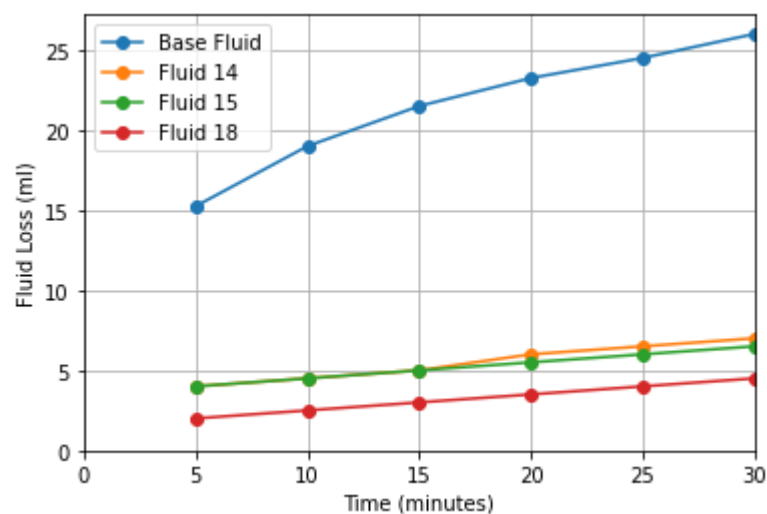


Figure 3.2.6 Fluid Loss for Base Fluid and fluids with added starch, cellulose and Calcium carbonate version 1.

Figure 3-2-6 are constructed the same as Fluids 13, 16 and 17 in Figure 3-2-5 with exception of the added starch. Fluid 14 contains 3,5g N-Dril HT and 3,5g Dextrid-E. The same goes for Fluid 15 that contains 3,5g N-Dril HT and 3,5g Dextrid-E and 5g Auracoat UF. Fluid 18 is constructed the same as Fluid 15 but with addition of 40g CaCO<sub>3</sub>, 20g CaCO<sub>3</sub> (<53µm) and 20g CaCO<sub>3</sub> (D50=50µm). When the concentrations of the two different fibres are equal, the results show very little difference in filtrate volume for Fluid 14 and 15.

However, when 40g of calcium carbonate is added, the results show a decrease in filtrate volume. This indicates that there are more particles in the drilling fluid, forming a tighter seal.

*Table 3.2 Filter Cakes for Base Fluid and Fluids containing different concentration of Calcium carbonate.*

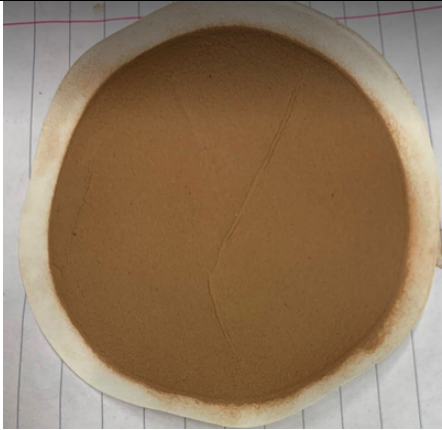





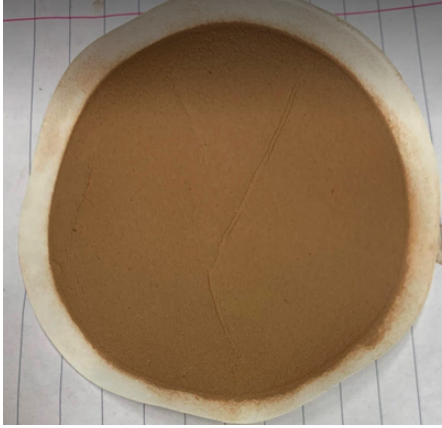





 <p><b>Base Fluid</b></p>	 <p><b>Sample 2</b></p>
 <p><b>Sample 6</b></p>	 <p><b>Sample 8</b></p>
 <p><b>Sample 9</b></p>	 <p><b>Sample 10</b></p>

Table 3.3 Filter Cakes for Base Fluid and fluids containing starch.

 <p><b>Base Fluid</b></p>	 <p><b>Sample 11</b></p>
 <p><b>Sample 12</b></p>	 <p><b>Sample 13</b></p>
 <p><b>Sample 16</b></p>	 <p><b>Sample 18</b></p>

### 3.3 Thermal and Mechanical Wear

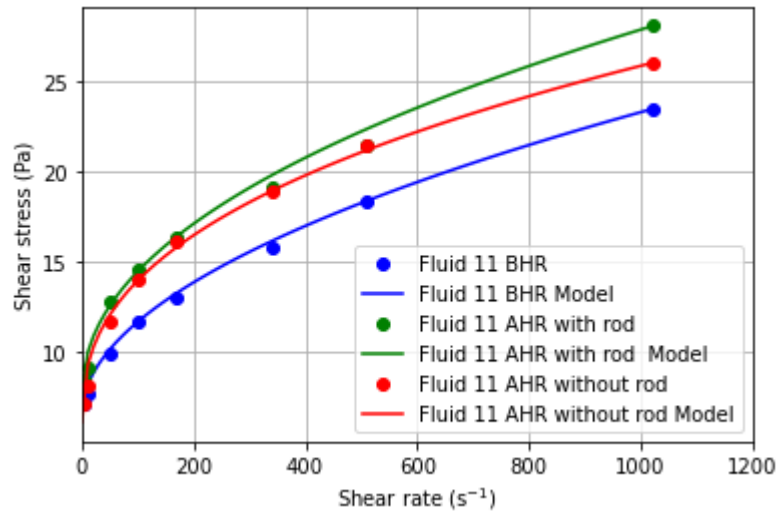


Figure 3.3.1 Flow Curves of the fluids with added N-Dril-HT BHR and AHR with and without steel rod.

Figure 3-3-1 shows Fluid 11 which contains 2g of N-Dril-HT Before Hot Rolling (BHR) and After Hot Rolling (AHR). To simulate mechanical wear during circulation a threaded steel rod is added into the cells during Hot Rolling (Klungtvedt and Saasen, 2022a) as shown in Figure 2.1.2. Fluid 11 AHR with a threaded steel rod has a larger increase in viscosity than Fluid 11 AHR without a threaded steel rod. Bergsvik (2022) found that fibre particles did not show any sign of particle degradation AHR, so a possible reason for the increase in viscosity AHR with a steel rod is enhanced interaction between N-Dril HT polymers because of the mechanical wear from the threaded steel rod.

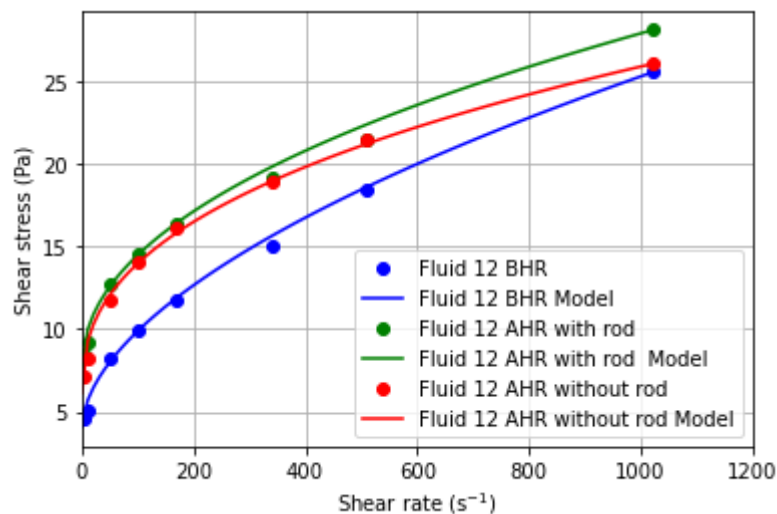


Figure 3.3.2 Flow Curves of the fluids with added Dextrid-E BHR and AHR with and without steel rod.

Figure 3-3-2 shows Fluid 12 which contains 5g of Dextrid-E Before Hot Rolling (BHR) and After Hot Rolling (AHR). Fluid 12 AHR without steel rod has a lower viscosity at high shear rates than fluid 11 from Figure 3-3-1. Dextrid-E, being a starch-based viscosifier, may be more prone to degradation AHR compared to N-Dril HT, which is a high-temperature resistant starch. Starch-based viscosifiers like Dextrid-E often exhibit shear-thinning behaviour, where the viscosity decreases with increasing shear rates. However, when the steel rod is introduced in Fluid 12 there is no decrease in viscosity. Mechanical wear can induce alignment of the polymer chains in the drilling mud. This alignment enhances the entanglement and interaction between the polymer chains, resulting in increased viscosity.

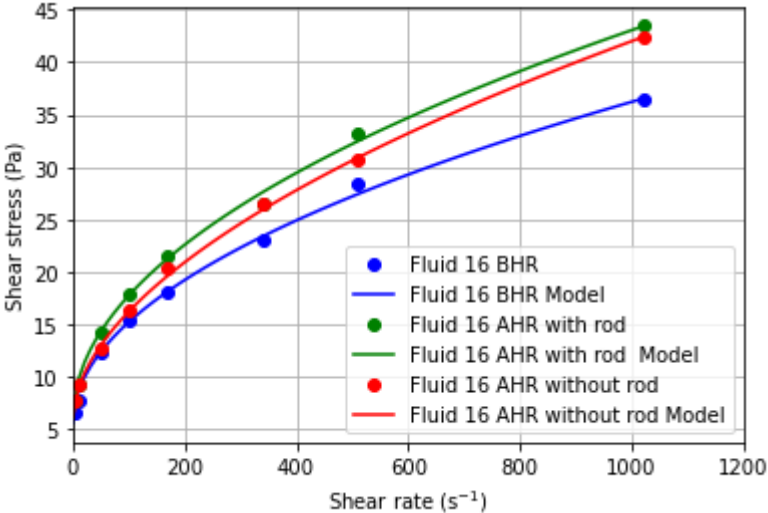


Figure 3.3.3 Flow Curves of the fluids with added starch and Calcium carbonate BHR and AHR with and without steel rod.

Figure 3-3-3 shows Fluid 16 which contains 2g N-Dril HT, 5g of Dextrid-E and 40g CaCO<sub>3</sub> Before Hot Rolling (BHR) and After Hot Rolling (AHR). Figure 3-3-3 depicts Fluid 16, which consists of 2g of N-Dril HT, 5g of Dextrid-E, and 40g of CaCO<sub>3</sub> before and after Hot Rolling (BHR and AHR). The addition of CaCO<sub>3</sub> results in a smaller difference between the cell with a threaded steel rod and the cell without. One possible reason for this is that temperature during Hot Rolling plays a more crucial role for calcium carbonate. Research conducted by Souza et al. (2022) found that temperature had the most significant impact on LCM effectiveness, with higher temperatures leading to larger volumes of filtrate. However, Fluid 16 with a threaded steel rod in the Hot Rolling cell exhibits slightly higher viscosity compared to the cell without the rod. This finding aligns with the results presented in Figure 3-3-2, where mechanical wear induces alignment of the polymer chains in the drilling mud. The alignment of polymer chains can contribute to increased viscosity. It should be noted that the behavior of Fluid 16 and the influence of Hot Rolling can be influenced by various



factors, including the concentration and properties of N-Dril HT, Dextrid-E, and CaCO<sub>3</sub>, as well as the specific conditions of the Hot Rolling process.

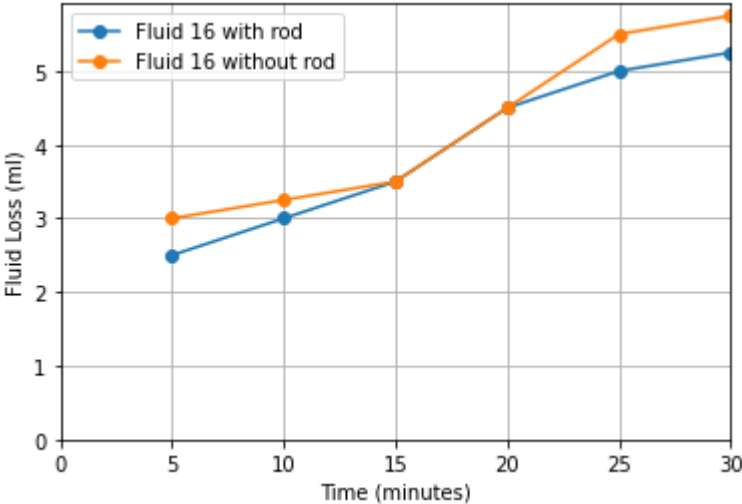


Figure 3.3.4 Fluid Loss for Fluid 16 AHR with and without steel rod.

Figure 3-3-4 presents the Fluid Loss for Fluid 16 with and without mechanical wear. The results indicate that Fluid 16 without mechanical wear exhibits slightly higher fluid loss compared to Fluid 16 with mechanical wear. These findings align well with the viscosity measurements conducted in Figure 3-3-3. Water-based mud (WBM) supplemented with fibres and calcium carbonate results in the formation of a tight filter cake. Klungvedt and Saasen (2023) discovered that the analysis of filter cake formation indicated that the external filter cake played a dominant role in controlling the fluid loss in their conducted tests. The same can be said for this study, where the filter cake is the predominant factor influencing the Fluid Loss tests.

## 4 Sources of Error

It is important to consider uncertainty in scientific experiments, as it can have a significant impact on the results. If the uncertainty is greater than the effects of the different LCMs, it cannot be concluded that the LCMs have any influence, as the result may solely be due to the uncertainty associated with the experiment. To ensure reliable results in the experimental section of the thesis, it is necessary to conduct repeatable experiments with minimal variations between them. To achieve this goal, it is essential to minimize the human variables in each experiment. Additionally, between each experiment, all equipment is thoroughly cleaned to maintain uniform conditions for each trial. The equipment uncertainties are listed in Appendix E. The viscometer is calibrated using a calibration fluid presented in Appendix C, and the result shows a deviation of 0.2 cP. Appendix E includes a table of five measurements performed on the Base Fluid without added LCM before and after Hot Rolling, and the average is calculated. This average value is used to determine the total uncertainty of the experiment by employing formulas 4.1 and 4.2.

- Human error
  - Human errors can occur during the reading of viscosity: If the sample is not read correctly on the viscometer, it can lead to incorrect viscosity results.
  - The reading of Fluid Loss is subject to human errors. Samples with high Fluid Loss require switching of the cylinder tube when it gets filled up to a new one, during which a few drops may get lost and the reading of fluid loss in mL may be incorrect.
- Equipment
  - In this thesis, the Ofite 800 viscometer is used, which has no temperature control. The tests are performed at room temperature, but the temperature may vary by a few degrees Celsius from parallel to parallel. Viscosity is temperature-dependent, so differences in temperature can affect the measurements between the parallels and can yield different results.
  - For the dimensions of R1B1 the minimum spring factor (F) is 1.0, for these dimensions the viscometer gives stable readings from 100-600 rpm but at the lower rates 100-3 rpm the readings are less stable (Appendix D).
  - From Appendix C, a deviation of 0.2 cP was found when a calibration fluid was used.
- Lesson Learned
  - Fritoli et al (2021) found that the pH range for drilling fluids is usually 8 to 12, but for Xanthan Gum solutions they are stable inside the 4 to 11 pH range. At a pH of 12 and higher, Xanthan Gum degrades after Hot Rolling, and the viscosity is significantly affected. In the initial measurements, the pH was too high, and the amount of xanthan gum was too low. Therefore, the amount of xanthan gum was increased, and the pH was decreased to prevent excessive degradation of xanthan gum after Hot Rolling and to avoid a drastic decrease in viscosity in the rest of the thesis.

$$\text{Uncertainty}[\%] = \frac{\text{standard deviation}}{\text{mean}} * 100\% \quad (4.1)$$

$$\text{Total standard deviation} = \sqrt{\sum \sigma_i^2} \quad (4.2)$$

*Table 4.1 Base Fluid Before Hot Rolling (Appendix G) and its uncertainties.*

Rotational Speed [rpm]	Mean Deflection, $\theta$ (1-5)	Standard Deviation, $\sigma$	Uncertainty. %
600	41,9	0,341	0,814
300	32,6	0,374	1,147
200	28,2	0,224	0,794
100	23,2	0,245	1,056
60	20,2	0,245	1,213
30	17,3	0,600	3,468
6	13,7	0,245	1,788
3	12,7	0,245	0,019

*Table 4.2 Base Fluid After Hot Rolling (Appendix G) and its uncertainties*

Rotational Speed [rpm]	Mean Deflection, $\theta$ (1-5)	Standard Deviation, $\sigma$	Uncertainty. %
600	49,8	0,748	1,502
300	39,0	0	0
200	33,5	0,316	0,943
100	27,3	0,245	0,897
60	24,3	0,245	1,008
30	21,0	0	0
6	15,0	0	0
3	13,6	0,200	1,470

## 5 Economic Overview and Environmental Accounting

### 5.1 Economic Overview

This thesis offers the advantage of being cost-effective to reproduce. The required equipment, including the Ofite viscometer, LPLT filter press, Hamilton Beach mixer, and Mettler Toledo scale, are commonly available in laboratories, minimizing additional expenses. In particular, the LPLT filter press proves to be a cost-effective and user-friendly alternative to an HPHT test. This thesis utilizes a water-based drilling fluid, which is easily producible and incorporates additives that are commonly accessible in most laboratories. The production of water-based drilling mud is relatively inexpensive. The addition of various LCMs (Lost Circulation Materials) and  $CaCO_3$  (calcium carbonate) is both cost-effective and readily available. The fibres and cellulose additives used in this study have been given by the European mud company for testing purposes. However, they can be substituted with similar LCMs possessing equivalent properties. Overall, this thesis offers an economically viable approach by utilizing readily available equipment, cost-effective drilling fluid components, and the potential for substitution of additives, allowing for affordable reproduction and testing in various laboratory settings. WBM fluids are cheap compared to OBM, Oil-based Mud, (Shaida, 2020), therefore there is a compelling economic incentive to enhance the characteristics of water-based mud.

### 5.2 Environmental Accounting

The production process of water-based drilling mud, incorporating additives such as caustic soda, barite, MgO, NaCl, xanthan gum, soda ash, water, and additional components like LCM  $CaCO_3$ , N-Dril HT, Dextrid-E, and cellulose bridging agent Auracoat UF, can be analysed from an environmental perspective. According to SINTEF and Statoil's (2014) environmental assessment report, the acute toxicity of water-based drilling fluids is generally low due to the classification of most additives as posing little or no effects to the environment (PLONOR). Although the main components in water-based drilling fluid are not considered toxic, the particles may have some physical effect on the planktonic and benthic organisms. Such consequences are local, generally within a range of a maximum of 100 m from the drilling location (Statoil 2016). Options for the disposal of WBM drill cuttings include discharge to sea, reinjection and skip and ship for disposal onshore (Corallian 2022). In the laboratory where WBM is produced, proper waste disposal and sorting procedures are implemented. At the University of Stavanger, there is a strong emphasis on waste sorting and management. In line with environmental accounting principles. This waste sorting process ensures that potentially hazardous or non-recyclable materials are segregated and disposed of safely, minimising the environmental impact.

## 6 Conclusion

The key findings of this thesis are:

- Fluids containing larger particle sizes of calcium carbonate ( $CaCO_3$ ) exhibited slightly higher values for yield stress and surplus stress. This can be attributed to increased particle interactions due to larger surface areas.
- The addition of higher concentrations of calcium carbonate and starch increased the viscosity of the fluids at higher shear rates. The shear thinning index (n) also became larger for fluids with higher concentrations of solid particles.
- There is a critical concentration of calcium carbonate where the viscosity starts to decrease instead of increasing. Fluid 10, containing 60g of  $CaCO_3$ , had lower viscosity compared to other samples.
- The addition of Auracoat UF, a cellulose-based bridging agent, enhanced the bridging capability of the fluid, resulting in higher yield stress and surplus stress values.
- Hot Rolling with a threaded steel rod resulted in increased viscosity, possibly due to mechanical wear can also promote stronger interactions between polymer molecules and other particles or additives in the drilling mud.
- The presence of fibres, calcium carbonate, and Hot Rolling contributed to the formation of a solid filter cake, reducing fluid loss.
- The addition of fibres and calcium carbonate in water-based mud promotes the formation of a solid filter cake, which contributes to lower fluid loss.
- The thesis offers a cost-effective approach with readily available equipment and drilling fluid components, allowing for affordable reproduction and testing in various laboratory settings.
- The environmental impact of water-based drilling mud is generally low, with additives classified as posing little or no effects on the environment. Proper waste disposal and sorting procedures are implemented in the laboratory to minimize environmental impact.
- Human errors can occur during viscosity readings and fluid loss measurements, potentially leading to inaccurate results.

## 7 References

- Halvorsen, H., Blikra, H.J., Grelland, S.S., Saasen, A. and Khalifeh, M. 2019. Viscosity of Oil-Based Drilling Fluids, *Ann. Trans. Nordic Rheol. Soc.*, **27**, 77-85. Lowry, T., Winn, C.,
- Dobson, P., Samuel, A., Kneafsey, T., Bauer, S., Ulrich, C. (2022). Examining the Monetary and Time Costs of Lost Circulation., *Proceedings 47nd, Workshop on Geothermal Reservoir Engineering*, Stanford University.
- Alsaba, M., Nygaard, R., Saasen, A., Nes, O. M. (2014). Lost Circulation Materials Capability of Sealing Wide Fractures. SPE-170285-MS. [https://www.researchgate.net/publication/281178135\\_Review\\_of\\_Lost\\_Circulation\\_Materials\\_and\\_Treatments\\_with\\_an\\_Updated\\_Classification](https://www.researchgate.net/publication/281178135_Review_of_Lost_Circulation_Materials_and_Treatments_with_an_Updated_Classification)
- Alsaba, M., Nygaard, R., Hareland, G. (2014b). Review of Lost Circulation Materials and Treatments with an Updated Classification. *2014 AADE Fluids Technical Conference and Exhibition*, Houston, TX, Apr. 15–16, Paper No. AADE-14-FTCE-25
- Fritoli, G. d. S., De Lai, F. C., Junqueira, S. L. D. M. (2021). Effect of LCM and polymeric additives on mudcake and filtrate rheology parameters. *Journal of Petroleum Science and Engineering*, <https://doi.org/10.1016/j.petrol.2021.108948>
- Grelland, S. S., (2021). Analysis of lost circulation on the Norwegian Continental Shelf. M.Sc. thesis, University of Stavanger.
- Bergsvik, S. I., (2022). Optimizing formulations for reservoir drilling fluids. B.Sc. thesis, University of Stavanger.
- Jeennakorn, M., Alsaba, M., Nygaard, R. *et al.* (2019). The effect of testing conditions on the performance of lost circulation materials: understandable sealing mechanism. *J Petrol Explor Prod Technol* **9**, 823–836. <https://doi.org/10.1007/s13202-018-0550-4>
- Klungtvedt, K. R., & Saasen, A. (2022a). Comparison of Lost Circulation Material Sealing Effectiveness in Water-Based and Oil-Based Drilling Fluids and Under The Conditions of Mechanical Shear and High Differential Pressure. *Journal of Energy Resources Technology*, **10**. <https://doi.org/https://doi.org/10.1115/1.4054653>
- Yang, M., Li, M. C., Wu, Q., Growcock, F. B., Chen, Y. (2020). Experimental study of the impact of filter cakes on the evaluation of LCMs for improved lost circulation preventive treatments. *Journal of Petroleum Science and Engineering*, Houston, USA, **191** (2020), pp. 107-152. <https://doi.org/10.1016/j.petrol.2020.107152>
- Souza, T. M., Filho, M. N. B., Calçada, L. A., Scheid, C. M. (2022). Evaluation of the effect of temperature and pressure on the process of combating loss of circulation using fibrous and

granular materials. *Journal of Petroleum Science and Engineering*. 219, <https://doi.org/10.1016/j.petrol.2022.111115>

Power, D. & Zamora, M. (2003). Drilling Fluid Yield Stress: Measurement Techniques for Improved Understanding of Critical Drilling Fluid Parameters. Paper AADE-03-NTCE-35, *AADE 2003 National Technology Conference*, Houston.

Klungtvedt, K. R., & Saasen, A. (2022b). Invasion of CaCO<sub>3</sub> Particles in Porous Formations in Presence of fibres. *Journal of Petroleum Science and Engineering*, 215. <https://doi.org/https://doi.org/10.1016/j.petrol.2022.110614>

Klungtvedt, K. R. & Saasen, A. (2023). The Role of Particle Size Distribution for Fluid Loss Materials on Formation of Filter-Cakes and Avoiding Formation Damage. *Journal of Energy Resources Technology*. 145(4). <https://doi.org/10.1115/1.4056187>

Saasen, A. Ytrehus, J. D. (2020). Viscosity Models for Drilling Fluids—Herschel-Bulkley Parameters and Their Use. *Journal Energies*. 13(20), 5271; <https://doi.org/10.3390/en13205271>

Corallian Energy Limited (2022). Victory Field Development Environmental Statement. [https://assets.publishing.service.gov.uk/government/uploads/system/uploads/attachment\\_data/file/1089579/Corallian\\_Victory\\_Development\\_ES-2022-003\\_06Jul22\\_Redacted.pdf](https://assets.publishing.service.gov.uk/government/uploads/system/uploads/attachment_data/file/1089579/Corallian_Victory_Development_ES-2022-003_06Jul22_Redacted.pdf)

Statoil Petroleum (2016). Utgard Environmental Statement. <https://www.equinor.com/content/dam/statoil/documents/impact-assessment/utgard/statoil-utgard-environmental-statement-may-2016.pdf>

Statoil Petroleum AS & SINTEF. (2014). Dispersion Modeling, Resource Mapping and Environmental Assessment. <https://www.sintef.no/contentassets/fdfb76c6b1db40729b9a96c17fbc902e/dispersion-modeling-resource-mapping-and-environmental-assessment.pdf>

PET210. University of Stavanger. (2022). Exercises in Drilling and Well Fluids

Shaida, A. (2020). Advantages and Disadvantages of Water and Oil-Based Mud. <https://www.linkedin.com/pulse/advantages-disadvantages-water-oil-based-mud-abu-shaida>

All sources used in this thesis are properly cited.



## 8 Appendix A

Table 8.1: A-1 Name of mixtures and added different size Calcium carbonate concentration.

Sample Number	Referred to as:	Name of fluid in recipe in Appendix
1	Base Fluid + CaCO <sub>3</sub> (<23 $\mu$ m)	Sample 1
2	Base Fluid + CaCO <sub>3</sub> (<53 $\mu$ m)	Sample 2
3	Base Fluid + CaCO <sub>3</sub> (D50=50 $\mu$ m)	Sample 3
4	Base Fluid + CaCO <sub>3</sub> (<23 $\mu$ m) + CaCO <sub>3</sub> (<53 $\mu$ m)	Sample 4
5	Base Fluid + CaCO <sub>3</sub> (<23 $\mu$ m) + CaCO <sub>3</sub> (<53 $\mu$ m) + CaCO <sub>3</sub> (D50=50 $\mu$ m)	Sample 5

Table 8.2 A-2: Name of mixtures with different Calcium carbonate concentration for size <53 $\mu$ m.

Sample Number	Added CaCO <sub>3</sub> in grams	Name of fluid in recipe in Appendix
2	20	Sample 2
6	40	Sample 6
7	45	Sample 7
8	50	Sample 8
9	55	Sample 9
10	60	Sample 10

Table 8.3 A-3: Name of mixtures and added different starch sample 11-16.

<b>Sample Number</b>	<b>Referred to as:</b>	<b>Name of fluid in recipe in Appendix</b>
11	Base Fluid + N-Dril HT	Sample 11
12	Base Fluid + Dextrid-E	Sample 12
13	Base Fluid + N-Dril HT + Dextrid-E Version 1	Sample 13
14	Base Fluid + N-Dril HT + Dextrid-E Version 2	Sample 14
15	Base Fluid + N-Dril HT + Dextrid-E + Auracoat UF Version 2	Sample 15
16	Base Fluid + N-Dril HT + Dextrid-E + Auracoat UF Version 1	Sample 16

Table 8.4 A-4: Name of mixtures and added different starch and Calcium carbonate

<b>Sample Number</b>	<b>Referred to as:</b>	<b>Name of fluid in recipe in Appendix</b>
17	Base Fluid + N-Dril HT + Dextrid-E + Auracoat UF + CaCO <sub>3</sub> Version 1	Sample 17
18	Base Fluid + N-Dril HT + Dextrid-E + Auracoat UF + CaCO <sub>3</sub> Version 2	Sample 18

## 9 Appendix B

Table 9.1 B-1: Recipe and mixing sequence for samples 1-3 in grams unless stated otherwise.

	Base Fluid	Sample 1	Sample 2	Sample 3	Sample 4	Sample 5
Sample Size	350 (mL)	350 (mL)	350 (mL)	350 (mL)	350 (mL)	350 (mL)
Water	335,49	328,08	328,08	3328,08	320,68	313,27
Soda Ash	0,02	0,02	0,02	0,02	0,02	0,02
Caustic Soda	0,25	0,25	0,25	0,25	0,25	0,25
XC	2	2	2	2	2	2
MgO	1	1	1	1	1	1
NaCl	20	20	20	20	20	20
Barite	20	20	20	20	20	20
CaCO <sub>3</sub> (<23 $\mu$ m)	0	20	0	0	20	20
CaCO <sub>3</sub> (<53 $\mu$ m)	0	0	20	0	20	20
CaCO <sub>3</sub> (D50=50 $\mu$ m)	0	0	0	20	0	20

*Table 9.2 B-2: Recipe and mixing sequence for samples 11-16 in grams unless stated otherwise.*

	<b>Sample 11</b>	<b>Sample 12</b>	<b>Sample 13</b>	<b>Sample 14</b>	<b>Sample 15</b>	<b>Sample 16</b>
Sample Size	350 (mL)	350 (mL)	350 (mL)	350 (mL)	350 (mL)	350 (mL)
Water	333,39	330,23	328,12	328,12	323,02	323,12
Soda Ash	0,2	0,2	0,2	0,02	0,2	0,02
Caustic Soda	0,25	0,25	0,25	0,25	0,25	0,25
XC	2	2	2	2	2	2
MgO	1	1	1	1	1	1
NaCl	20	20	20	20	20	20
Barite	20	20	20	20	20	20
Starch N - Dril HT	2	0	2	3,5	3,5	2
Starch Dextrid-E	0	5	5	3,5	3,5	5
Auracoat UF	0	0	0	0	5	5

Table 9.3 B-3: Recipe and mixing sequence for samples 18-19 in grams unless stated otherwise.

	<b>Sample 18</b>	<b>Sample 19</b>
Sample Size	350,00	350,00
Water	315,41	316,99
Soda Ash	0,02	0,02
Caustic Soda	0,25	0,25
XC	2	2
MgO	1	1
NaCl	20	20
Barite	20	20
CaCO <sub>3</sub> (<23 $\mu$ m)	0	0
CaCO <sub>3</sub> (<53 $\mu$ m)	20	20
CaCO <sub>3</sub> (D50=50 $\mu$ m)	20	20
Starch N - Dril HT	5	3,5
Starch Dextrid-E	2	3,5
Auracoat UF	5	5



## Calibration of viscometer - OFITE 93-99 Model 800 8-Speed

Date: 18.01.2023

Performed by: Karoline Sele / Jorunn H. Vrålstad

Place: 6

s/n: 93-99

VWR Water-Resistant/Shock-Resistant and Waterproof/Shockproof Stopwatch

- Accuracy 0,01%

Temperature [°C] : 20,4

- Thermometer Clas Ohlson article number 36-1833
  - Range from -50 °C to 300 °C
  - Accuracy of  $\pm 1$  °C for temperatures between -30 °C to 250 °C

Speed Accuracy [rpm]= 0,1

- For the dimensions of R1B1 the minimum spring factor (F) is 1.0, for these dimensions the viscometer can measure fairly well from 100-600 rpm but at the lower rates 100-3 rpm the readings are shaky.

Measurements of components:

- Rotor Sleeve - R1:
  - Rotor Radius: 1,8415 cm
  - Rotor diameter: 3,683 cm
- Bob - B1
  - Bob Radius: 1,7245 cm
  - Bob diameter: 3,449 cm
  - Bob height: 3,8 cm
- Torsion Spring - F1.0
  - Shear Stress Constant for Effective Bob Surface  $k_s$  [m<sup>3</sup>]= 0.01323
  - Overall Instrument Constant K= 300
  - Minimum Spring Factor (F) for R1B1= 1,0

Table 10.2 C-2: Measurements of calibration fluid.

600 rpm	300 rpm	200 rpm	100 rpm	60 rpm	30 rpm	6 rpm	3 rpm	Calculated [cP]	Expected [cP]
210	105	70,5	36,5	22	11,5	3	2	105	105,2

Calculations of cP:  $PV = \theta 600 - \theta 300$

Comments: The deviation of 0,2 cP is acceptable and will not have a significant impact on the accuracy requirements of the measurements.

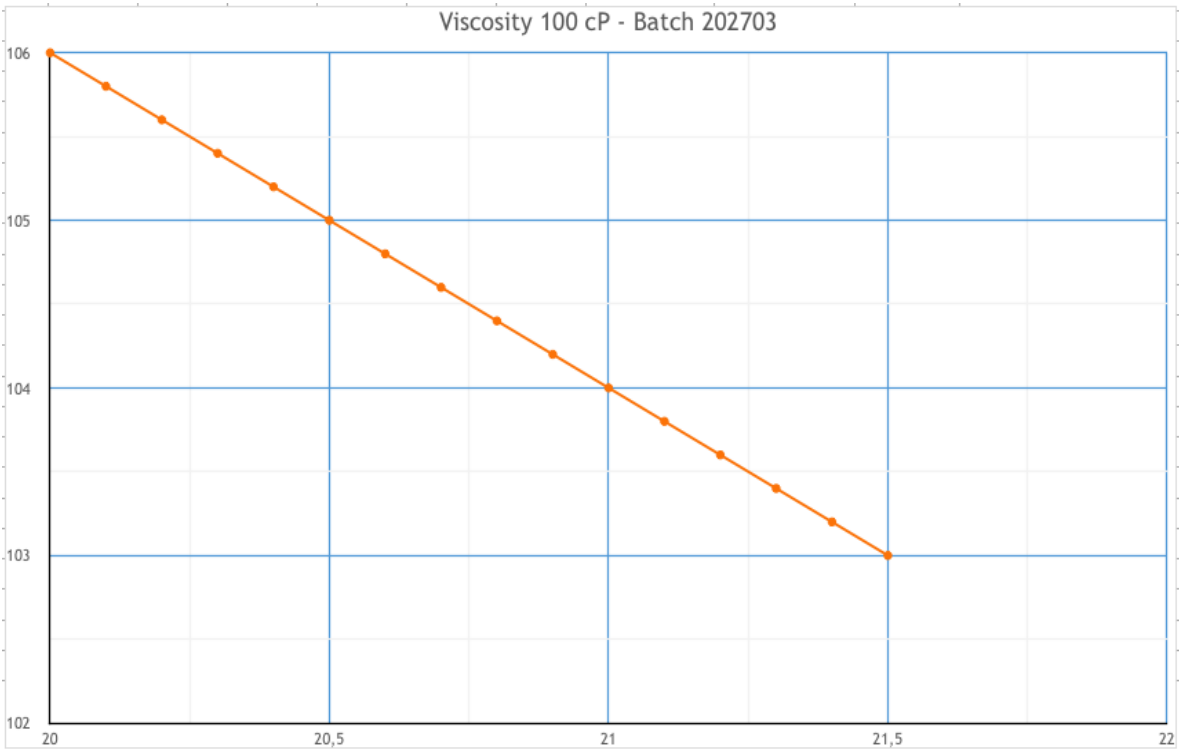


Figure 5.2.1 C-1: Measurements of calibration fluid.



## 11 Appendix D

ANSI/API Recommended practice 13B-1 Fifth Edition 2017

Follow the API procedure:

Determination of viscosity and gel strengths using a direct reading viscometer.

1. The drilling fluid is placed in the annular space between two concentric cylinders. The outer cylinder is called the rotor sleeve and it is driven at a constant rotational velocity. As the rotor sleeve rotates in the drilling fluid, it creates a torque on the inner cylinder, the bob. The movement of the bob is restrained by a torsion spring, and a dial attached to the bob indicates the displacement of the bob. By measuring the displacement of the bob, the viscometer is able to calculate the viscosity of the drilling fluid.
2. The components need to meet the ANSI/API specifications:
  - a. Rotor Sleeve - R1
    - i. Inside diameter: 36,83 mm
    - ii. Total length: 87,0 mm
  - b. Bob - B1
    - i. Diameter: 34,49 mm
    - ii. Cylinder length: 38,0 mm
  - c. Torsion Spring - F1.0
    - i. Torsional stiffness: 10,54 N\*m/rad
    - ii. Shear stress constant: 29,3 pascals per radian of deflection
  - d. Rotor sleeve speeds
    - i. High speed: 600 r/min
    - ii. Low speed: 300 r/min
3. Stopwatch
  - i. Accuracy 0,01%
4. Thermometer
  - a. Range from 0 °C to 105 °C and accuracy of  $\pm 1$  °C
5. Procedure
  - a. A sample of drilling fluid is filled into a cup. 50-100 mL of empty volume is left in the cup for displacements of fluid due to the bob and sleeve of the viscometer. Immerse the rotor sleeve exactly to the scribed line inside the cup. The sample needs to be cooled to the selected temperature, and mixed to obtain a uniform sample temperature. In this thesis the drilling fluid is Hot rolled for 16 hours at 90 °C, the drilling fluid then needs to cool down to room temperature and mixed for 10 minutes in a Hamilton Beach mixer before going into the viscometer. Measure and record the temperature of the drilling fluid before testing begins.
  - b. When the sleeve is rotating at 600 rpm, wait until the dial reaches steady state value to record the value.

- c. Reduce rotor speed to 300 rpm, 200 rpm, 100 rpm, 60 rpm, 30 rpm, 6 rpm and 3 rpm and follow the same procedure as 5b. It is important that the measurements of dial readings are performed stepwise from highest to lowest speed.
- d. Set the speed to 600 rpm again and wait until steady state. Stop the rotor and let the drilling fluid stand undisturbed for 10 seconds, use a stopwatch. Record the maximum reading when switching to 3 rpm speed, this is the initial gel strength ( $\beta_{10s}$ ).
- e. Re-stir the drilling fluid at 600 rpm until steady state value and stop the rotor and let the drilling fluid stand undisturbed for 10 minutes. Record the maximum reading when switching to 3 rpm speed, this is the gel strength after 10 minutes ( $\beta_{10m}$ ).

The dimensions for R1B1F1.0 determine the following:

- 1° deflection of the bob = shear stress 0,511 Pa = 1,067 lbf/100\*ft<sup>2</sup>
- 1 r/min of the rotor = shear rate 1,7023 s<sup>-1</sup>
- Viscosity (cP) = shear stress (mPa) / shear rate (1/s)
  - at 300 rpm (shear rate = 511 s<sup>-1</sup>) the degree of reflection will correspond to viscosity expressed in millipascal\*seconds (centipoises)

Plastic viscosity, commonly known in the industry by the abbreviation PV, is a measure of a fluid's resistance to flow at a given shear rate. PV is the difference between the shear stress at a low shear rate and the yield point, the point where the fluid begins to flow. This means that PV is the slope of the curve that relates to shear stress rate at shear rates below the yield point. To calculate PV from the readings of the viscometer the following formula is used:

$$\eta_{PV} = R_{600} - R_{300}$$

$$\eta_{PV} = \text{The plastic viscosity [cp] or [mPa * s]}$$

$$R_{600} = \text{The dial reading at 600 rpm [degrees of deflection]}$$

$$R_{300} = \text{The dial reading at 300 rpm [degrees of deflection]}$$

The yield point is the stress at which the material begins to deform plastically, this means that the material deforms permanently even after the stress is removed. To calculate the yield point expressed in pascals the following formula is used:

$$Y_{P,SI} = 0,511 \times (R_{300} - \eta_{PV})$$

$$Y_{P,SI} = \text{The yield point [Pa]}$$

$$R_{300} = \text{The dial reading at 300 rpm [degrees of deflection]}$$

$$\eta_{PV} = \text{The plastic viscosity [cp] or [mPa * s]}$$

The apparent viscosity, commonly known in the industry by the abbreviation AV, is a measure of the resistance of a fluid to flow. It is called "apparent" viscosity because it is a calculated value that takes into account the effect of shear rate on the measured viscosity. Apparent viscosity is a common way to express the viscosity of non-Newtonian fluids. To calculate AV from the readings of the viscometer the following formula is used:

$$\eta_{AV} = \frac{R_{600}}{2}$$

$\eta_{AV}$  = The apparent viscosity [cp] or [mPa \* s]

$R_{600}$  = The dial reading at 600 rpm [degrees of deflection]

### Determination of fluid loss on a Low-temperature/Low-pressure Filtrate Test

#### 1. Filter press

- a. Consisting mainly of a cylindrical drilling fluid cell having an inside diameter of 76,2 mm and height of at least 64,0 mm. The cell is made of materials resistant to strongly alkaline solutions and is so fitted that the pressure medium can be conveniently admitted into, and bled from, the top. A 90mm diameter filter paper can be placed in the bottom of the cell, just above a suitable support.
- b. The filtration area is  $45,8 \text{ cm}^2 \pm 0,6 \text{ cm}^2$
- c. The inner diameter of the filter press gasket determines the dimensions of the filtration area
  - i. Maximum diameter 76,86 mm
  - ii. Minimum diameter 75,86 mm

#### 2. Equipment

- a. Electronic or Mechanical timer
  - i. with 30 minutes interval
- b. Graduated cylinder
  - i. volume om 10 mL or 25 mL

#### 3. Procedure

- a. Measure and record the initial temperature of the drilling fluid to the nearest degree Celcius.
- b. Assemble the cell by placing a gasket in the base cap, place the screen on top of the gasket. Place the filter paper on top of the screen, and then place the sealing gasket on top of the paper. Finally assemble the cell. Pour the drilling fluid sample into the cell, to within 12 mm on the top and complete assembly.
- c. Place a clean dry graduated cylinder under the drain tube to collect the filtrate. Close the relief valve and adjust the regulator so that the pressure of  $100 \text{ psi} \pm 5 \text{ psi}$  is applied within 30 seconds or less.
- d. Start the 30 minute timer immediately at the time of pressure application.
- e. At the end of the 30 minute-test period, measure and record the filtrate volume.

- i. Reading the meniscus correctly is extremely important.
  - 1. Always read the meniscus with the interface at eye level.
  - 2. For the air-to-liquid meniscus read the lowest point of the meniscus which is in the middle and at the very bottom of the liquid.
- f. Shut off the flow through the pressure regulator and open the relief valve. The time interval shall be reported.

## 12 Appendix E

### Procedure

1. Mixing of the drilling fluid following the recipe.
2. Measure pH and Temperature.
3. Measure rheology with a viscosimeter.
4. Hot Roll the cell at 90 °C for 16 hours.
5. Cool down the cells to room temperature.
6. Mix the sample for 10 minutes with a Hamilton Beach Mixer
7. Measure pH and Temperature
8. Measure rheology with a viscosimeter.
  - Measure deflection at speeds 600, 300, 200, 100, 60, 30, 6 and 3 rpm
7. Conduct a LPLT test
  - Measure filtrate Volume in mL at point in time of 5, 10, 15, 20, 25 and 30 min.

## 13 Appendix F

*A list of the equipment used in this thesis:*

1. OFITE 93-99 Model 800 8-Speed Viscometer
  - a. Speed Accuracy [rpm]= 0,1
  - b. R1B1 F1.0
2. Thermometer Clas Ohlson article number 36-1833
  - a. Range from -50 °C to 300 °C
  - b. Accuracy of  $\pm 1$  °C for temperatures between -30 °C to 250 °C
3. VWR Water-Resistant/Shock-Resistant and Waterproof/Shockproof Stopwatch
  - a. Accuracy 0,01%
4. LTLP, low-pressure low-temperature test
  - a. 100 psi
5. Hamilton Beach Mixer
  - a. Spindle speed high: 23,900 rpm
  - b. Spindle speed medium: 21,800 rpm
  - c. Spindle speed low: 16,300 rpm
6. Mettler Toledo PB1502-S/FACT
  - a. Capacity of 1510g
  - b. Readability of 0.01g
  - c. Linearity of 0.02g
7. OFITE Roller Oven 172-00-1-RC
  - a. Temperature Range: 100 - 450°F (38 - 232.2°C)
  - b. Capable of maintaining a temperature of 150° F  $\pm$  5° F (65° C  $\pm$  3° C)
8. Threaded steel rod used in Hot Rolling
  - a. Biltema article number: 19-396
    - i. FZB, M16 x 2 mm
  - b. Pitch: 2 mm
  - c. length: 135 mm

## 14 Appendix G:

Measurements of Base Fluid without LCM:

*Table 14.1 G-1: Base Fluid Before Hot Rolling*

	<b>1</b>	<b>2</b>	<b>3</b>	<b>4</b>	<b>5</b>	<b>Mean (1-5)</b>
pH	12,5	12,5	12,6	12,4	12,3	12,46
Temp	25,1	25	24,6	25,7	25,4	25,16
600	42	41,5	41,5	42,5	42	41,9
300	32,5	32	32,5	33	33	32,6
200	28	28	28	28,5	28,5	28,2
100	23	23	23	23,5	23,5	23,2
60	20	20	20	20,5	20,5	20,2
30	16,5	17	17	18	18	17,3
6	13,5	13,5	13,5	14	14	13,7
3	12,5	12,5	12,5	13	13	12,7

Table 14.2 G-2: Base Fluid After Hot Rolling

	<b>1</b>	<b>2</b>	<b>3</b>	<b>4</b>	<b>5</b>	<b>Mean (1-5)</b>
pH	12,5	12,5	12,6	12,4	12,3	12,46
Temp	27,5	26,5	27	28	26	27
600 rpm	51	50	50	49	49	49,8
300 rpm	39	39	39	39	39	39
200 rpm	33	33,5	34	33,5	33,5	33,5
100 rpm	27	27,5	27,5	27	27,5	27,3
60 rpm	24	24,5	24,5	24,5	24	24,3
30 rpm	21	21	21	21	21	21
6 rpm	15	15	15	15	15	15
3 rpm	13,5	14	13,5	13,5	13,5	13,6

Table 14.3 G-3: Fluid Loss Base Fluid.

<b>Time (min)</b>	<b>Fluid Loss (mL)</b>
5	15,25
10	19
15	21,5
20	23,25
25	24,5
30	26



## 15 Appendix H

Article published at the Nordic Rheology Conference 2023:

### **THE EFFECT OF LOST CIRCULATION MATERIAL ON HERSCHEL-BULKLEY PARAMETERS**

Karoline Sele<sup>1</sup>, Jorunn H. Vrålstad<sup>1</sup>, Karl Ronny Klungtvedt<sup>2</sup> and Arild Saasen<sup>1</sup>

1: University of Stavanger, Stavanger, Norway

2: EMC AS, Stavanger, Norway

#### **ABSTRACT**

To hinder loss of drilling fluids into downhole formations while drilling geothermal, CO<sub>2</sub> injection or petroleum wells, lost circulation material (LCM) is added to the drilling fluids. These materials consist of many granular, fibrous, and flaky materials. The current article contains an assessment of the addition of fresh and worn granular and cellulose fibre based LCM on the viscous properties of drilling fluids. The viscosity is described as Herschel-Bulkley fluids using dimensionless shear rates. The viscosity data is combined with data on the LCM's ability to alter filtration loss.

#### **FUNCTIONS OF DRILLING FLUIDS AND THEIR PERFORMANCE UNDER ACTUAL WELL CONDITIONS**

Drilling fluid is one of the main components when drilling wells, and it has several important functions. One of the primary roles of drilling fluid is to control pore pressure and prevent leakage while also preventing the influx of formation water and gases into the wellbore. During drilling, the tools are subjected to high temperatures and pressures, and the drilling fluid helps to cool the tools and provide necessary lubrication to prevent overheating. As the drilling fluid flows through the drill bit nozzles, it is subjected to mechanical stress, high pressure, and high velocity, resulting in aeration, which occurs when the drilling fluid mixes with air or gas. The temperature in the well can also impact the drilling fluid through thermal degradation. Increased temperature in the formation can alter the chemical and physical composition of the drilling fluid, causing it to expand, increase pressure, reduce viscosity, or form foam, resulting in increased wear and tear on the drill bit and nozzles. To determine the behavior of drilling fluid under actual well conditions, it is essential to test it at high temperatures and during circulation through nozzles, simulating the relevant well conditions. Hot-rolling is one method used to simulate thermal wear and tear. However, hot-rolling alone cannot provide information on wear and tear associated with circulation in the borehole. To address this limitation, Klungtvedt and Saasen<sup>1</sup> describes a method that involves hot-rolling with a threaded steel rod placed in the cells while rolling at 90 degrees for 16 hours. This new approach enables more comprehensive assessment of a drilling fluid's performance in borehole conditions. The results showed that mechanical degradation had a significant impact on the sealing ability of the drilling fluid.

To hinder loss of drilling fluid to a porous or a fractured formation, lost circulation material (LCM) can be added to the drilling fluid. Calcium carbonate is one of the most commonly used additives as LCM and is easily available and cost-effective as it can be obtained both naturally and synthetically. This mineral is alkaline and increases the pH value when dissolved in water, which helps prevent corrosion of drilling tools and reduces the risk of formation damage. Calcium carbonate contributes to increasing the effective density of the drilling fluid, which helps maintain pressure in the formation and may increase oil and gas recovery. Another advantage of using calcium carbonate is improved formation water control. N-Dril HT is a

highly crosslinked starch and Dextrid E is a crosslinked starch, commonly used in drilling fluids to reduce fluid loss. N-Dril HT is a high-temperature resistant starch while Dextrid E is another starch based viscosifier. Auracoat UF is a patented mixture of cellulose fibre used to hinder fluid loss and formation damage.

The addition of starch and fibres to drilling fluids increases the viscosity of these fluids. This is advantageous as it then affects the particle carrying capacity of the liquid, allowing it to more effectively transport drill cuttings and waste from the wellbore to the surface. Increased viscosity can also help reduce fluid loss from the wellbore, thereby reducing the risk of formation damage. Calcium carbonate is ideal for use as a LCM in low-permeability formations, as it can create a gel when mixed with water to effectively seal leaks. It is most effective in water-based circulating fluids but can also be used in low-pressure formations. Incorporating fibres into drilling fluids is beneficial in wells where the fluid properties need improvement, such as high-temperature or formation damage-prone wells, or where increased viscosity is needed to enhance carrying capacity.

## **MATERIALS AND EXPERIMENTAL PROCEDURES**

In this article multiple tests were performed on a water-based drilling fluid with different LCM added. The recipes created by Sele<sup>5</sup>, which are included in Appendix. Following the recipes, all components were weighed on a Mettler Toledo scale. Once all components were added, the speed is set to high and mixed for 10 minutes. The mixture was then transferred into cells for hot-rolling. The cells are hot-rolled for 16 hours at 90 degrees Celsius. Subsequently, they are then cooled down to room temperature before being mixed again for 10 minutes at high speed. Finally, viscosity tests are conducted using an Ofite 800 viscometer.

Viscosity tests were performed in a viscometer with cup and bob geometry in accordance with oilfield standards<sup>2,3</sup>. To perform the test, the viscometer cup was filled with drilling fluid. This container was rotated at speeds of 600, 300, 200, 100, 60, 30, 6, and 3 rpm, corresponding to shear rates of 1022, 511, 340.7, 170.3, 102.2, 51.1, 10.2 and 5.11 1/s. All measurements were recorded after the values had stabilised. All tests were conducted in descending order of speed. After completing the viscosity tests, the gel strength of the fluid was measured by first setting the speed to 600 rpm and allowing it to stand for 15 seconds. The speed was then reduced to zero and the fluid was left to stand still for 10 seconds before the speed was set to 3 rpm and the highest reading was recorded. This process was repeated with a waiting time of 10 minutes before the viscometer was set to 3 rpm and the following peak measurement was recorded.

The experimental procedure involved placing the cell in a filter press under ambient conditions of temperature and pressure, with measurements recorded at 5-minute intervals over a 30-minute duration as per the API standard. To accurately quantify fluid loss, a filter paper with a pore size of 2.2  $\mu\text{m}$  was employed to conduct a fluid loss test on drilling fluids containing fibres of varying sizes. This particular pore size was deemed optimal efficient capture of drilling fluid particles and fibres, while allowing for unimpeded fluid flow to ensure precision in measurement. Utilisation of a filter paper with a thicker pore size could result in blockages and hence, inaccurate measurements of fluid loss.

## **THE HERSCHEL-BULKLEY MODEL**

The Herschel-Bulkley model is the most widely used viscosity model for drilling fluids due to its ability to provide reasonably accurate predictions over a broad range of shear rates. This model incorporates both Power-law behaviour and yield stress as shown in Eq. 1.

$$\tau = \tau_0 + k(\dot{\gamma})^n \quad (1)$$

In Equation 1, the Herschel-Bulkley model is defined with three parameters:  $k$ ,  $n$ , and  $\tau_y$ , representing the consistency index, flow behaviour index and yield stress, respectively.

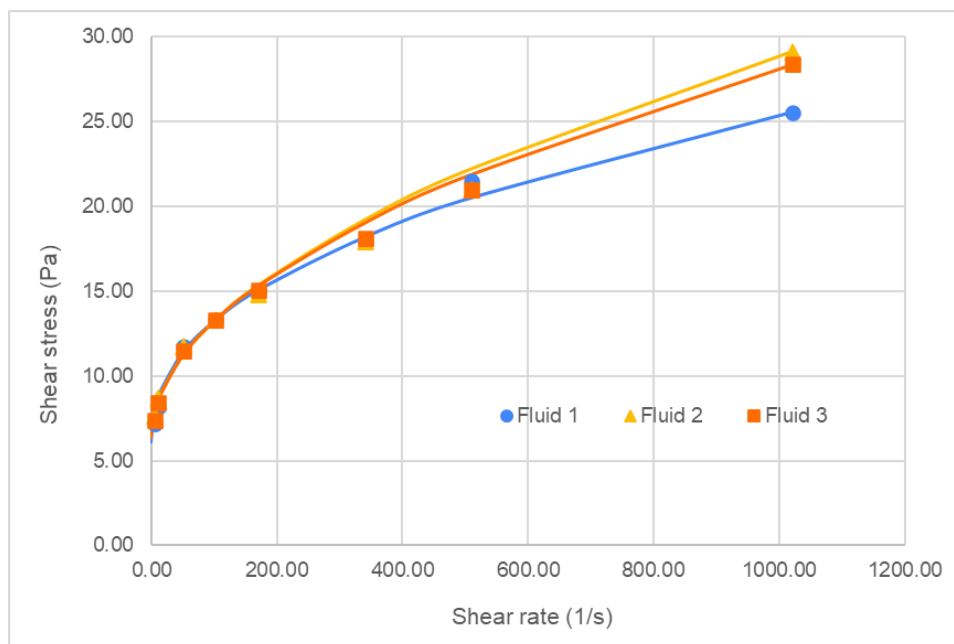
However, using these parameters in comparing fluids can be challenging because the consistency index,  $k$ , is not directly related to viscosity but is dependent on the flow behaviour index,  $n$ , i.e.,  $k=k(n)$ . To address this issue, Saasen and Ytrehus<sup>4</sup> developed a modified model based on a model by Nelson and Ewoldt<sup>5</sup>. This modified model, presented in Eq. 2, uses dimensionless shear rates to provide independent parameters.

$$\tau = \tau_y + \tau_s \left( \frac{\dot{\gamma}}{\dot{\gamma}_s} \right)^n \quad (2)$$

In the following,  $\tau_y$  is determined using a linear regression of the 5.11 and 10.22 1/s readings as suggested by Power and Zamora<sup>6</sup>,  $\tau_s$  is determined at 102.2 1/s and  $n$  is determined at 1022 1/s.

## RESULTS AND DISCUSSIONS

**Fig. 1** shows the plot of the viscosity measurement data for samples 1, 2, and 3. With the exception of carbonate content, these fluids were constructed equally. Sample 1, 2 and 3 had 20, 40 and 60 g calcium carbonate per 350 mL respectively. The yield stress, surplus stress, and  $n$ -value were calculated using Eq. 2. From the data shown in **Fig. 1**, it seems that addition of the two larger concentration of calcium carbonate only added to the viscosity of the fluid at higher shear rates. In Table 1 it is tabulated the Herschel-Bulkley parameters for dimensionless shear rates for these fluids. It is seen that the shear thinning index,  $n$ , became a bit larger for Sample 2 and 3. This is expected as the amount of solid particles became higher for these fluids giving a high shear rate viscosity.

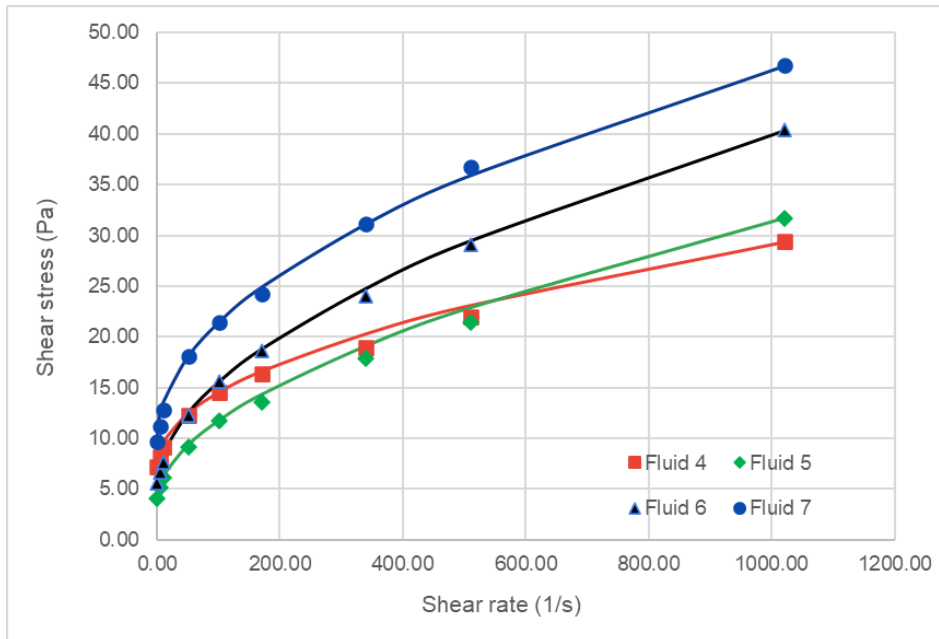


**FIGURE 1:** Flow curve of Sample 1, 2 and 3 with three different concentrations of CaCO<sub>3</sub>. Solid line is their Herschel-Bulkley parameters.

The measurements shown in **Fig. 1** provide insights into the behaviour of drilling fluids if no fibres are added to the fluids. The results from the experiments demonstrate that Sample 2, containing both the smaller and larger size particles of calcium carbonate, exhibits the highest viscosity readings on the viscometer. This can be attributed to the fact that the two different particle sizes can fill the voids between each other, resulting in a denser and more stable structure. Another important factor is the increase in the amount of added calcium carbonate from 20 grams to 60 grams, which also has an impact on the viscosity of the drilling fluid.

**Table 1:** Dimensionless shear rate based Herschel-Bulkley parameters of Samples 1, 2 and 3.

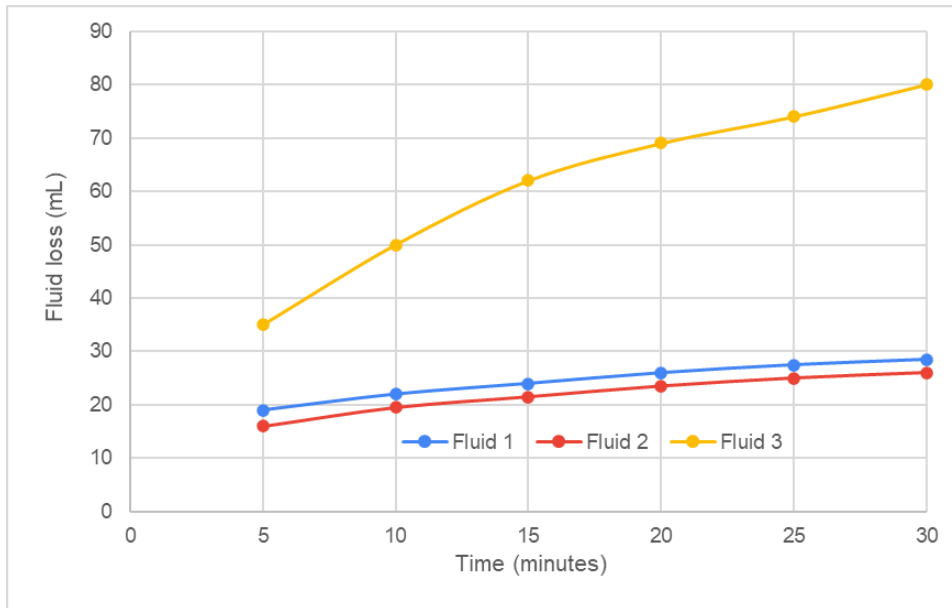
	Yield Stress	Surplus Stress	$n$
Sample 1:	6.132	7.154	0.43
Sample 2:	6.643	6.643	0.53
Sample 3:	6.388	6.899	0.50



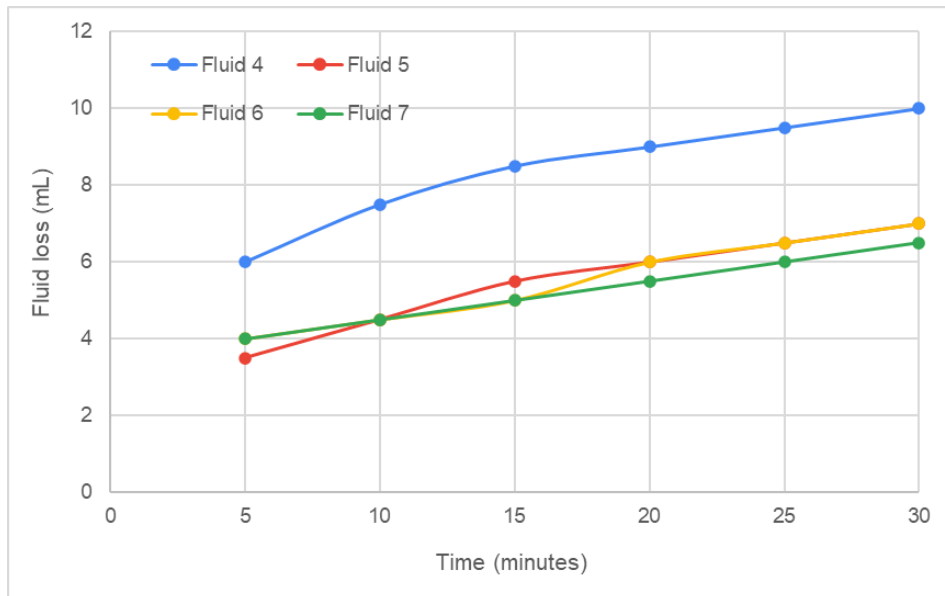
**FIGURE 2:** Flow curves of the fluids with added starch.

A series of drilling fluids with addition of starch is shown in **Fig. 2**. The total concentration of addition of starch and fibres increased in this series. Fluid 4 had the lowest concentration of starch, in this case N-Dril-HT. Exchanging 2g N-Dril-HT with 5g Dextrid E resulted in a reduction in low shear viscosity and an increase in high-shear viscosity. Further addition of starch and fibres resulted in an overall increase in viscosity.

The results shown in **Fig. 3** shows the effect of calcium carbonate on fluid loss. The fluid loss increases when the CaCO<sub>3</sub> particles are too large, as the filter cake is not packed tightly enough. Additionally, the fluid loss is higher when the drilling fluid is only supplemented with calcium carbonate, as opposed to when starch is added as shown in **Fig. 4** Furthermore, when starch and Auracoat UF are added, the fluid loss decreases even further. The inclusion of cellulose fibres in drilling fluids enhances the binding of polymers to the filter cake, leading to reduced release of polymers into the formation. This could be attributed to the polar properties of both cellulose particles and polymers, which potentially lead to increased inter-particle adhesive and frictional forces. While the fluid loss tests in this study were conducted at 100 psi, Klungtvedt and Saasen<sup>7</sup> discovered that the most significant variations in Fluid Loss, attributed to the use of N-Dril-HT cross linked starch and Dextrid E modified starch in conjunction with Auracoat UF, which is a cellulosic fibre mixture, were observed at pressure ranges of 500-1000 psi.



**FIGURE 3:** Fluid Loss test for base fluid with three different sizes of CaCO<sub>3</sub>.



**FIGURE 4:** Fluid Loss test for base fluid with added starch

## CONCLUSIONS

A series of experiments shows that some starch polymers provide better fluid loss control than calcium carbonate, at least as long as the test pressure is as described in oilfield standards. The variation in viscosity was significant when the drilling fluid polymer content was varied. The viscosity of the fluids was less sensitive to the calcium carbonate content.

## REFERENCES

1. Klungtvedt, K. R. and Saasen, A. Comparison of Lost Circulation Material Sealing Effectiveness in Water-Based and Oil-Based Drilling Fluids and Under The Conditions of Mechanical Shear and High Differential Pressure, *J. Energy Res. Techn.*, 10 2022., <https://doi.org/https://doi.org/10.1115/1.4054653>
2. International Organization for Standardization: *Petroleum and natural gas industries – Field testing of drilling fluids. Part 1: Water-based fluids*, Report ISO 10414-1, Geneva, 2008

3. International Organization for Standardization: *Petroleum and natural gas industries – Field testing of drilling fluids. Part 2: Oil-based fluids*, Report ISO 10414-2, Geneva, 2011
4. Saasen, A. and Ytrehus, J.D. Rheological Properties of Drilling Fluids – Use of Dimensionless Shear Rates in Herschel-Bulkley Models and Power-Law Models, *Applied Rheology*, **28** (5), paper 54515, 2018. DOI:10.3933/ApplRheol-28-54515
5. Nelson A.Z. and Ewoldt R.H. Design of yield stress fluids: A rheology-to-structure inverse problem, *Soft Matter*, **13**, 7578-7594, 2017.
6. Power D. and Zamora M. Drilling Fluid Yield Stress: Measurement Techniques for Improved Understanding of Critical Drilling Fluid Parameters. Paper AADE-03-NTCE-35, AADE 2003 National Technology Conference, Houston, 2003.
7. Klungtvedt, K. R. and Saasen, The Role of Particle Size Distribution for Fluid Loss Materials on Formation of Filter-Cakes and Avoiding Formation Damage, *J. Energy Res. Techn.*, 2023

## APPENDIX

*Recipe for the fluids. All values in gram.*

	Sample 1	Sample 2	Sample 3	Sample 4	Sample 5	Sample 6	Sample 7
Sample size	350	350	350	350	350	350	350
Water	328,08	320,68	313,27	333,39	330,23	328,12	323,02
Soda Ash	0,02	0,02	0,02	0,2	0,2	0,2	0,2
Caustic Soda	0,25	0,25	0,25	0,25	0,25	0,25	0,25
XC	2	2	2	2	2	2	2
MgO	1	1	1	1	1	1	1
NaCl	20	20	20	20	20	20	20
Barite	20	20	20	20	20	20	20
CaCO <sub>3</sub> (<23µm)	20	20	20	0	0	0	0
CaCO <sub>3</sub> (<53µm)	0	20	20	0	0	0	0
CaCO <sub>3</sub> (D50=50µm)	0	0	20	0	0	0	0
Starch N - Dril HT	0	0	0	2	0	2	3,5
Starch Dextride - E	0	0	0	0	5	5	3,5
Auracoat UF	0	0	0	0	0	0	5

## 16 Appendix I

*Python codes made by Karoline Sele.*

### **I-1 Modified Herschel-Bulkley model.**

Python code where the user can input experimental values in degrees and obtain a graph with the experimental values and the modified Herschel-Bulkley model from equation 1.3:

```
import matplotlib.pyplot as plt
import numpy as np

# Fluid data
fluids = ['Base Fluid', 'Fluid 1', 'Fluid 2', 'Fluid 3'] #write the name of the fluids
rpm_values = [600, 300, 200, 100, 60, 30, 6, 3]

# Conversion factors
rpm_to_s = 1.7023
deg_to_Pa = 0.511

# User input of degree values
degree_values = {}
colors = ['blue', 'green', 'red', 'orange'] # Define colors for each fluid
for fluid, color in zip(fluids, colors):
    degree_values[fluid] = [float(input(f"Enter degree value for {fluid} at {rpm} rpm: ")) for
rpm in rpm_values]
    degree_values[fluid + '_color'] = color # Store color for each fluid

# Calculate experimental values in Pa and s-1
exp_values = {}
for fluid in fluids:
    exp_values[fluid] = {
        'x': [rpm * rpm_to_s for rpm in rpm_values],
        'y': [degree * deg_to_Pa for degree in degree_values[fluid]],
        'color': degree_values[fluid + '_color'] # Assign color to experimental values
    }

# Calculate models for each fluid
models = {}
for fluid in fluids:
    # Calculate  $\tau_y$ 
    tau_y = (2 * exp_values[fluid]['y'][7]) - (exp_values[fluid]['y'][6])
```

```

# Calculate  $\tau_s$ 
tau_s = exp_values[fluid]['y'][4] - tau_y

# Calculate n
n = (np.log((exp_values[fluid]['y'][0] - tau_y)) - np.log(tau_s)) / (np.log(1022 * rpm_to_s) -
np.log(102.2 * rpm_to_s))

# Calculate model values
model_x = np.linspace(0, 1021.38, 100) # Upper limit of x-axis
model_y = tau_y + tau_s * (model_x / (60 * rpm_to_s)) ** n

models[fluid] = {'x': model_x, 'y': model_y}

# Print the calculated values
print(f"Fluid: {fluid}")
print(f"n: {n}")
print(f" $\tau_y$ : {tau_y}")
print(f" $\tau_s$ : {tau_s}")
print()

# Plot data and models
plt.figure()
for fluid in fluids:
    plt.plot(exp_values[fluid]['x'], exp_values[fluid]['y'], 'o', label=fluid,
color=exp_values[fluid]['color'])
    plt.plot(models[fluid]['x'], models[fluid]['y'], '-', label=f"{fluid} Model",
color=exp_values[fluid]['color'])
plt.xlim([0, 1200]) # Set the x-axis limit to 1200 s-1
plt.xlabel('Shear rate (s-1)')
plt.ylabel('Shear stress (Pa)')
plt.grid(True) # Add grid lines
plt.legend()
plt.show()

```



## I-2 Fluid Loss.

*Python code where the user can input experimental values in mL and obtain a graph with the experimental values for Fluid Loss:*

```
import matplotlib.pyplot as plt

# Fluid data
fluids = ['Fluid 1', 'Fluid 2', 'Fluid 3', 'Fluid 4']
times = [5, 10, 15, 20, 25, 30] # Times in minutes

# User input of fluid loss values
fluid_loss = {}
for fluid in fluids:
    fluid_loss[fluid] = [float(input(f"Enter fluid loss (ml) for {fluid} at {time}
minutes: ")) for time in times]

# Plot data
plt.figure()
for fluid in fluids:
    plt.plot(times, fluid_loss[fluid], 'o-', label=fluid)

plt.xlabel('Time (minutes)')
plt.ylabel('Fluid Loss (ml)')
plt.legend()
plt.xlim([0, 30]) # Upper limit for x-axis
plt.ylim(bottom=0) # Set y-axis minimum to 0
plt.grid(True) # Add gridlines
plt.show()
```